ELSEVIER

Inorganica Chimica Acta 235 (1995) 215–231

Inorganica Chimica Acta

Synthetic methodologies for tripodal phosphines. The preparation of $MeSi(CH_2PPh_2)_3$ and $n\text{-}BuSn(CH_2PPh_2)_3$ and a comparison of their rhodium(I) and ruthenium(II) coordination chemistry. The X-ray crystal structures of $[Rh(NBD)\{n\text{-}BuSn(CH_2PPh_2)_3\}](OTf)$ and $[Rh(NBD)\{MeSi(CH_2PPh_2)_3\}](OTf)$ ☆

Susanna Herold [a], Antonio Mezzetti [a,1], Luigi M. Venanzi [a,*], Alberto Albinati [b], Francesca Lianza [b], Tobias Gerfin [c], Volker Gramlich [c]

[a] *Laboratorium für Anorganische Chemie, Eidgenössische Technische Hochschule, Universitätstrasse 6, CH-8092 Zurich, Switzerland*

[b] *Istituto di Chimica Farmaceutica, Università di Milano, Viale Abruzzi 42, I-20131 Milan, Italy*

[c] *Institut für Kristallographie und Petrographie der Eidgenössischen Technischen Hochschule, Sonneggstrasse 5, CH-8092 Zurich, Switzerland*

Received 5 October 1994; revised 20 January 1995

Abstract

The preparation of the new tripodal ligands $MeSi(CH_2PPh_2)_3$ (Si-triphos) and $n\text{-}BuSn(CH_2PPh_2)_3$ (Sn-triphos) and their complexes of rhodium(I) of the type [Rh(NBD)(tripod)](OTf) (NBD = norbornadiene, OTf = triflate) and of ruthenium(II) of the type $[Ru(O_2CCF_3)_2(tripod)]$, is reported. The coordination chemistry of the new tripodal phosphines, and in particular that of Sn-triphos, differs significantly from that of $MeC(CH_2PPh_2)_3$ (triphos). A comparison of the X-ray structure of [Rh(NBD)(triphos)](OTf) with those of the new complexes [Rh(NBD)(Sn-triphos)](OTf) and [Rh(NBD)(Si-triphos)](OTf) shows that the steric requirements of the ligands $RE(CH_2PPh_2)_3$ (E = C, Si and Sn), increase from the carbon to the tin compound. The coordination chemistry of ruthenium(II) indicates that, relative to triphos, Sn-triphos displays an enhanced steric bulk which, however, is not sufficient to stabilize the mononuclear, five-coordinate dichloro complexes.

Keywords: Tripodal phosphine complexes; Rhodium complexes; Ruthenium complexes; Crystal structures; Silicon compounds; Tin compounds

1. Introduction

Tripodal polyphosphines have proved to be useful and versatile ligands for most transition metals [1,2]. In particular, the coordination chemistry of $MeC(CH_2PPh_2)_3$ (triphos) (**1**) has been very extensively investigated since the first report of its preparation in 1963 [3]. Furthermore, several studies have shown that **1** is a useful and versatile ligand in organometallic chemistry [1,4]. The coordination chemistry of triphos is still a topic of current interest [5,6] and, recently, its transition-metal complexes have received even more attention because of their activity in several homogeneously catalyzed reactions, e.g. hydrogenation [6,7b], hydroformylation [7], acetalization [8], oxidation [9], oligomerization [10] and desulfurization [11].

Newer developments in this area have included the preparation of C_3 homochiral analogues of triphos [12]. Studies in this laboratory [12a,c,e,f] and elsewhere [12b,d], have been directed to the preparation of tripodal phosphines having chirality at the P atoms with the aim of carrying out some of the above-mentioned catalytic reactions enantioselectively, in order to compare the catalytic properties of transition-metal complexes containing C_3-symmetric tripodal ligands with the corresponding systems with C_2-symmetric bidentate ligands, which have proved to be very successful for enantioselective catalysis [13].

The approach used in this laboratory [12a,c] for the preparation of optically pure $MeSi(CH_2P(t\text{-}Bu)Ph)_3$ (**2**) involved: (a) the synthesis of the racemic monodentate phosphine MeP(t-Bu)(Ph); (b) protection of its P atom

☆ This paper is dedicated to the memory of Professor Ugo Croatto.

* Corresponding author.

[1] On leave from Dipartimento di Scienze e Tecnologie Chimiche, Università di Udine, via del Cotonificio 108, I-33100 Udine, Italy.

0020-1693/95/$09.50 © 1995 Elsevier Science S.A. All rights reserved
SSDI 0020-1693(95)04474-N

as the borane adduct $MeP(BH_3)^tBuPh$; (c) its racemate resolution; (d) deprotonation of the methyl group of the optically pure phosphine borane; (e) coupling of the resulting carbanion with a suitable silicon compound to produce a tripodal framework; (f) deprotection of the P atoms by treatment of the phosphine borane with an amine (Scheme 1).

However, preliminary studies showed that, unlike the triphos complexes, the rhodium and ruthenium analogues containing ligand **2** did not show catalytic activity in a variety of test reactions [12a]. Furthermore, preliminary experiments using rhodium complexes of racemic (*RRR*+*SSS*)-$CH_3C(CH_2PMePh)_3$ (**3**) indicated that they are less active, particularly in Lewis acid catalyzed reactions, than the corresponding compounds containing triphos **1** [12a]. It was thus deduced that best efficiency was likely to be achieved when *two* terminal aryl substituents were present on each P atom. Efforts were then directed to developing a general method for the synthesis of tripodal phosphines of the type $RE(CH_2PArAr')_3$ which could be easily extended to the preparation of enantiopure C_3-symmetric ligands using the reaction sequence shown in Scheme 1. As can be seen there, this sequence requires the presence of a heteroatom E, i.e. Si, in the bridging position of the tripodal skeleton [12a,c,e,f] and, therefore, the influence of this heteroatom on the coordination chemistry of the resulting ligands had to be studied. The compound $MeSi(CH_2PPh_2)_3$ (**4**) was chosen as a model to be investigated prior to the synthesis of chiral tripodal phosphines of the type $MeSi(CH_2PArAr')_3$.

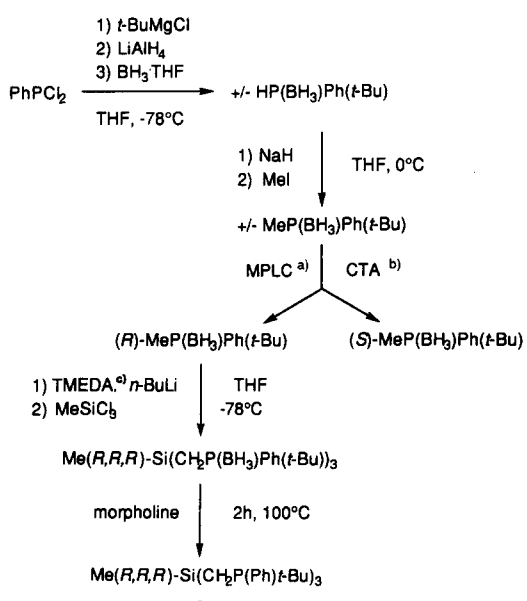

a) MPLC = medium pressure liquid chromatography; b) CTA = cellulose triacetate; c) TMEDA = *N,N,N′,N′*-tetramethylethylene diamine.

Scheme 1.

This paper reports unsuccessful attempts to prepare compound **4** by the route shown in Scheme 1. This route, however, allowed the preparation of its tin analogue n-$BuSn(CH_2PPh_2)_3$ (**5**). While compound **4** was eventually obtained by another route, this cannot be used to prepare optically pure ligands. A preliminary exploration of the coordination chemistry of these two ligands with rhodium(I) and ruthenium(II), which most directly relates to applications in homogeneous catalysis, is also described. The crystal structures of their rhodium derivatives [Rh(NBD)(Sn-triphos)](OTf) and [Rh(NBD)(Si-triphos)](OTf) (NBD = norbornadiene, OTf = triflate) are discussed and compared with that of the triphos analogue.

2. Results and discussion

2.1. Synthesis of the ligands

2.1.1. $MeSi(CH_2PPh_2)_3$, Si-triphos (4)

Attempts were made to prepare this ligand as shown in Scheme 2. The reaction of $MeSiCl_3$ with α-lithium methylenediphenylphosphine borane, $LiCH_2P(BH_3)Ph_2$ (**7**), prepared as described by Imamoto et al. [14], did not yield the expected trisubstituted methyl silane $MeSi(CH_2P(BH_3)Ph_2)_3$ (**8**) and only the starting material $MeP(BH_3)Ph_2$ (**6**) could be recovered in ~50% yield. This was unexpected as $MeSi(CH_2P(BH_3)Ph(^tBu))_3$ is easily formed by this route. Thus the failure to obtain **8** as shown above was investigated in detail.

The lithiation of the methyl group on the phosphine borane $MeP(BH_3)Ph_2$ (**6**), with formation of $LiCH_2P(BH_3)Ph_2$ (**7**), under the conditions used, was first checked. A slight excess (~10%) of *sec*-BuLi was added to a 0.3 M THF solution of phosphine borane **6** at −78 °C and an aliquot of the reaction mixture was neutralized with MeOD, after 2 h. This converted the lithiated methylphosphine borane **7** to the deuterated compound $CH_2DP(BH_3)Ph_2$ (**6a**), which was identified

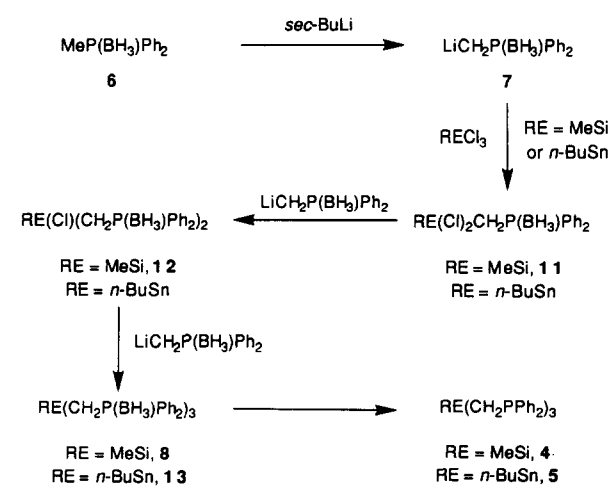

Scheme 2.

by its ^{1}H NMR spectrum. The integration of the ^{1}H NMR signals of **6** and **6a**, in the ^{1}H NMR spectrum of the reaction solution, revealed that the formation of **7** was practically quantitative.

In situ, NMR studies of the coupling step were then carried out. After deprotonation of the phosphine borane **6**, as described above, $MeSiCl_3$ was rapidly added to the reaction mixture at −78 °C. After warming up to room temperature, the ^{31}P NMR spectrum of the reaction mixture showed the presence of two products, together with a large amount (up to 50%) of methyldiphenylphosphine borane **6**. Heating of the reaction mixture, or allowing it to react for a longer time, or using an excess of the lithiated phosphine, gave the same results. Therefore, the failure to obtain compound **8** was attributed to a further reaction of one of the Si-intermediates formed, e.g. **11** or **12** in Scheme 2. Thus, some experiments with Me_2SiCl_2 and Ph_2SiCl_2 were carried out, the reactions being performed as described for the synthesis of **2** [12a,c]. The corresponding diphosphine boranes $Me_2Si(CH_2P(BH_3)Ph_2)_2$ (**9**) and $Ph_2Si(CH_2P(BH_3)Ph_2)_2$ (**10**) were formed in 90 and 70% yield, respectively. Thus, it appeared likely that the problem encountered with the preparation of **8** occurred during the third substitution step.

As shown in Scheme 2, the methylene group in intermediate **12** is placed between the P and Si heteroatoms and can be easily deprotonated as these substituents stabilize the resulting carbanion [15]. Therefore, two competing reactions can take place, i.e. the nucleophilic substitution of the chlorine atom of **12** to give compound **8**, and the *trans*-metallation reaction between the lithiated phosphine borane and silane **12**, shown in Eq. (1). The latter reaction leads to the regeneration of the original methylphophine borane **6** and, consequently, the third nucleophilic substitution at the silicon atom does not take place.

$$\underset{\mathbf{12}}{MeSi(Cl)(CH_2P(BH_3)Ph_2)_2} + \underset{\mathbf{7}}{LiCH_2P(BH_3)Ph_2} \longrightarrow MeSi(Cl)(CH(Li)P(BH_3)Ph_2)(CH_2P(BH_3)Ph_2) + \underset{\mathbf{6}}{MeP(BH_3)Ph_2} \quad (1)$$

The only difference between $CH_3P(BH_3)$(t-Bu)Ph and the phosphine borane **6** is the replacement of a t-butyl by a phenyl substituent on the P atom. These two groups have very different electronic properties: while t-butyl is electron-donating, the phenyl substituent is weakly electron-withdrawing. Consequently, the deprotonated form of an intermediate such as **12** is favoured when both substituents on the phosphine borane are aryl groups. This implies that the competing *trans*-metallation reaction is less likely during the formation of the siliphos borane $2(BH_3)_3$.

Several qualitative reactions were carried out using other trichlorosilanes, i.e. $PhSiCl_3$, t-$BuSiCl_3$ or $SiCl_4$. These showed that, even though the chosen trichlorosilanes did not contain any α-protons, they did not yield trisubstituted products in the nucleophilic substitution reaction with the lithium derivative **7**: after methanolysis the major component in each of these reactions was the methylphosphine borane **6**. This is a further indication that the *trans*-metallation reaction occurs between the lithiated phosphine borane **7** and intermediate **12** and does not involve the terminal methyl group.

An attempt to accelerate the nucleophilic substitution was carried out using the silyl tris(triflate) $MeSi(OTf)_3$ ($OTf = CF_3SO_3$) [16], instead of $MeSiCl_3$, as silyl triflates are widely employed in organic syntheses because of their high reactivity [17]. This reagent was conveniently prepared by the two-step route consisting of (i) the preparation of $MeSiCl(OTf)_2$ by cleavage of two phenyl groups from $MePh_2SiCl$ using CF_3SO_3H, and (ii) the abstraction of the chlorine atom with silver triflate from the chlorosilane $MeSiCl(OTf)_2$. This procedure gave the highly moisture-sensitive $MeSi(OTf)_3$ in 72% yield.

The coupling reaction between $MeSi(OTf)_3$ and **7**, carried out using the conditions given in Scheme 2, was indeed faster than with $MeSiCl_3$, as the ^{31}P NMR spectrum of the solution showed the formation of one major new product within 10 min. However, the only product which could be isolated by flash chromatography, after work-up of the reaction mixture was, once again, the phosphine borane **6** in a ~50% yield. No significant change in the product distribution was observed by running the reaction at higher temperatures.

Finally, the reactivity of other methylalkylarylphosphine boranes toward $MeSiCl_3$ was investigated. The aim of these qualitative experiments was to show that the success of the third coupling step directly depended on the nature of the other two substituents on the methylphosphine boranes. Thus, one of the methyl groups of dimethylphenylphosphine borane, $Me_2P(BH_3)$-Ph, and that of ethylmethylphenylphosphine borane, $EtMeP(BH_3)Ph$, were selectively deprotonated as described for **6**. Their coupling reactions with $MeSiCl_3$ gave the corresponding trisubstituted products: ^{31}P NMR spectroscopic studies showed that, in each case, the expected triphosphine was formed in 60–70% yield.

In conclusion, the experiments described above show that *three successive nucleophilic substitutions* on the silicon atom of $MeSiCl_3$ cannot be carried out using metallated methylphosphine boranes *unless at least one of the other two substituents on the P atom is an alkyl group.*

$$MeSi(CH_2Cl)_3 + 3LiPPh_2 \xrightarrow{-LiCl} \underset{\mathbf{4}}{MeSi(CH_2PPh_2)_3} \quad (2)$$

As the coordination chemistry of $MeSi(CH_2PPh_2)_3$ (**4**) was of interest in order to compare it with that of the corresponding C-ligand, triphos, an alternative synthetic route to **4** was followed (Eq. (2)). The reaction of a 90% pure fraction of $MeSi(CH_2Cl)_3$ [18] with lithium diphenylphosphide, at −10 °C, in THF solution, yielded analytically pure Si-triphos **4**, in 70% yield, after recrystallization from MeOH. The disadvantage of this method is that it cannot be used to prepare optically pure tripodal Si-phosphines. Ligand **4** proved to be of a stability comparable to that of triphos and its rhodium(I) coordination chemistry will be described later.

2.1.2. *n-BuSn(CH_2PPh_2)$_3$, Sn-triphos (5)*

A breakthrough, at the level of the coupling step, was achieved by substituting the silicon heteroatom with tin. The tripodal phosphine Sn-triphos **5** was successfully prepared as described in Scheme 2. The lithium derivative **7** reacted with n-$BuSnCl_3$ at −78 °C and gave the expected tripodal phosphine borane n-$BuSn(CH_2P(BH_3)Ph_2)_3$ (**13**) in 87% yield. n-$BuSnCl_3$ was prefered to $MeSnCl_3$ as (i) it is much less toxic than $MeSnCl_3$ and (ii) the differences in electronic and steric effects on the donor capacity of the P atoms between the ligands with the bridgehead n-butyl and methyl substituents should only be slight. Consequently, this choice should not influence the coordination chemistry of the resulting ligand. The free phosphine n-$BuSn(CH_2PPh_2)_3$ (**5**) was obtained in ~80% yield by removing the borane protecting groups from **13** with morpholine, using the procedure described by Imamoto et al. [14]. Phosphine **5** is a colourless oil at room temperature. Its solutions can be handled in air for limited periods of time without formation of significant amounts of phosphine oxides.

2.2. *The rhodium complexes*

2.2.1. *Synthesis of Rh(NBD)(X-triphos)](OTf) (X=Si (14), Sn (15))*

The synthesis of the complexes [Rh(NBD)(Si-triphos)](OTf) (**14**) and [Rh(NBD)(Sn-triphos)](OTf) (**15**) was carried out as described for the triphos analog [Rh(NBD)(triphos)](OTf) [6a]: the diolefin complex $[Rh_2Cl_2(NBD)_2]$, when treated with silver triflate, gave the solvento intermediate $[Rh(NBD)(S)_2]^+$ (S = acetone or acetonitrile) which was then reacted with the tripodal ligands **2** and **5** to give the complexes **14** and **15**, respectively, in almost quantitative yields.

2.2.2. *X-ray structures of [Rh(NBD)(X-triphos)](OTf) (X=Si (14), Sn (15))*

The crystals of **14** and **15** contain the discrete cations $[Rh(NBD)(Si\text{-triphos})]^+$ and $[Rh(NBD)(Sn\text{-triphos})]^+$, respectively, and triflate counterions. As the ORTEP views of these two cations are very similar, only that of the silicon compound **14** is shown in Fig. 1 [2]. A selection of bond lengths and angles in the cations $[Rh(NBD)(X\text{-triphos})]^+$ (X = Si (**14**), Sn (**15**)) are given in Table 1, together with those of the homologous cation of [Rh(NBD)(triphos)](OTf) (**16**) [19].

The coordination geometries of the cations in the Si-triphos and Sn-triphos derivatives, i.e. in **14** and **15**, respectively, resemble each other and can be regarded as distorted trigonal bipyramidal with P2 and the mid-point of the C4–C5 double bond (MP2) in the axial positions and P1, P3 and the double bond C1–C2 constituting the equatorial plane. In **14** and **15**, the P1, P3, C1 and C2 atoms are coplanar within 0.02 and 0.06 Å, the Rh atoms being displaced toward P2 by 0.08 and 0.12 Å, respectively. The axial P2 atoms form angles with the P1P3MP1 planes which are close to 90°. Although the mid-points MP2 are displaced from the *trans* axial positions, the P2–Rh–MP2 angles are uniquely the largest (~158°). However, the triphos analogue **16** can be better described on the basis of a square pyramidal geometry, with P3 in the axial position [19].

Both in **14** and in **15** the NBD double bond which lies in the equatorial plane (C1–C2) is closer to rhodium than the axially-bonded one (C4–C5). The Rh–MP1 and Rh–MP2 distances differ also in **16**, but the change is much smaller. In this context, it should be noted that the equatorial plane of a d^8 trigonal bipyramidal complex contains a well hybridized, doubly occupied d_π orbital which can strongly interact with the olefin π^* level [20], while this is not the case for the second double bond. This, moreover, is slightly off the main axis as a result of the small bite angle of the NBD molecule in the above cations (65–68°). However, the observed Rh–C distances are not unusual [21] and the magnitudes of the standard deviations do not allow a discussion of the C–C distances in the two types of double bonds. Electronic arguments also allow an interpretation of the differences observed in the Rh–P distances. In complexes **14** and **15**, the Rh–P1 and Rh–P3 equatorial distances are longer than the axial one Rh–P2, as expected for a σ-donor in a d^8 TBP structure [20]. In the triphos analogue **16**, there is a unique longest Rh–P3 distance which corresponds to the apical position of the square pyramid, in agreement with theoretical considerations on d^8 SPY transition-metal complexes [20].

Within the RhP1P2P3 moieties, the P–Rh–P bond angles increase from the triphos cation **16**, ~90°, to the corresponding silicon and tin species **14** and **15**, respectively, and reach ~94° in the latter compound. The opening of the P–Rh–P angles reflects the length-

[2] An ORTEP view of the cation in **15** is shown in Fig. S1, see Section 5.

Table 1
Selected interatomic distances (Å) and bond angles (°) in [Rh(NBD)(tripod)](OTf) (tripod = Si-triphos (**14**), Sn-triphos (**15**), triphos (**16**))

	Si-triphos, **14**	Sn-triphos, **15**	triphos, **16** [19]
Rh–P1	2.426(3)	2.445(4)	2.311(1)
Rh–P2	2.317(3)	2.336(3)	2.319(1)
Rh–P3	2.406(3)	2.400(4)	2.399(1)
Rh–MP1 [a]	2.05(1)	2.01(2)	2.055(9)
Rh–MP2 [b]	2.20(1)	2.14(2)	2.115(9)
Rh–C1	2.15(1)	2.12(1)	2.166(7)
Rh–C2	2.18(1)	2.13(1)	2.157(7)
Rh–C4	2.28(1)	2.27(1)	2.205(6)
Rh–C5	2.28(1)	2.24(1)	2.233(7)
C1–C2	1.40(2)	1.36(2)	1.33(1)
C4–C5	1.36(2)	1.40(2)	1.33(1)
E–C8	1.87(1) [c]	2.14(1) [d]	1.545(8) [e]
E–C9	1.90(1) [c]	2.16(1) [d]	1.553(7) [e]
E–C10	1.89(1) [c]	2.16(1) [d]	1.564(8) [e]
E–C11	1.84(1) [c]	2.09(2) [d]	1.535(8) [e]
P1–Rh–P2	92.5(1)	94.3(1)	87.8(1)
P1–Rh–P3	93.8(1)	94.5(1)	91.2(1)
P1–Rh–MP1 [a]	127.2(3)	123.9(4)	145.1(3)
P1–Rh–MP2 [b]	104.0(3)	102.8(5)	95.6(3)
P2–Rh–P3	90.9(1)	94.2(1)	87.1(1)
P2–Rh–MP1 [a]	92.4(4)	91.2(4)	99.0(3)
P2–Rh–MP2 [b]	157.1(4)	158.5(4)	158.0(3)
P3–Rh–MP1 [a]	138.7(4)	140.7(4)	123.2(3)
P3–Rh–MP2 [b]	103.7(4)	97.4(5)	114.5(2)
MP1–Rh–MP2	64.9(5)	68.4(5)	66.3(4)
C8–E–C9	106.2(5) [c]	101.0(4) [d]	111.2(4) [e]
C8–E–C10	110.5(5) [c]	105.2(4) [d]	113.5(4) [e]
C9–E–C10	108.4(5) [c]	102.2(4) [d]	111.1(4) [e]
Rh···E [f]	3.700(3) [c]	3.858(3) [d]	3.555(6) [e]
Rh···(P1,P2,P3) [g]	1.318(2)	1.273(4)	1.382(1)

[a] MP1 is the mid-point of C1–C2.
[b] MP2 is the mid-point of C4–C5.
[c] E = Si.
[d] E = Sn.
[e] E = C.
[f] Non-bonding distance between Rh and the heteroatom at the top of the tripod skeleton (E).
[g] Distance of the Rh atom from the plane defined by the three P atoms.

ening of the E–C bonds in the ligand framework on going from C (mean value 1.55 Å) to Sn (mean value 2.14 Å). The main consequence is that the metal centre becomes progressively more embedded in the tripod ligand cavity as its size increases. This is clearly shown by the position of the rhodium centre relative to the P1P2P3 plane, which is 1.38 Å in the triphos complex **16**, 1.32 Å in the Si-triphos compound **14**, and 1.27 Å in the Sn-triphos analogue. Therefore, the P atoms are closer to the NBD ligands in **14** and **15** than in **16**, and the inter-ligand steric crowding increases along the series **16** < **14** < **15**. This is reflected in the Rh–P distances, whose average value increases on going from **16** (mean value 2.32 Å) to **14** (mean value 2.38 Å) and to **15** (mean value 2.39 Å). However, all these distances fall within the reported Rh–P range [21].

The effect of changing the steric requirements of the tripodal ligand on the coordination geometry is highlighted in Fig. 2, which shows the projections of the three cations **14**, **15** and **16** along the Rh–E axes. In the triphos complex **16**, the orientation of the NBD ligand, relative to the RhP1P2P3 moiety, is such that the C1–C2 and C4–C5 double bonds are roughly perpendicular to the RhP1P2 basal plane, in agreement with a square pyramidal geometry with P3 in axial position. In this conformation P1 and P2 are eclipsed with C5 and C1, respectively, leading to short non-bonded contacts (P1···C5 and P2···C1 are 3.13 and 3.28 Å, respectively). Due to the higher steric bulk of Si- and Sn-triphos, compared wih triphos, such a geometry is expected to be disfavoured in **14** and **15**. Indeed, the P2RhC1C2 torsion angles of 107.1, 88.3 and 85.0° for **16**, **14** and **15**, respectively, indicate that in **14** and **15** the diolefins are tilted around the Rh–E axes, relative to the RhP1P2P3 moieties, as compared with **16**. The tilting of the NBD ligands, which minimizes

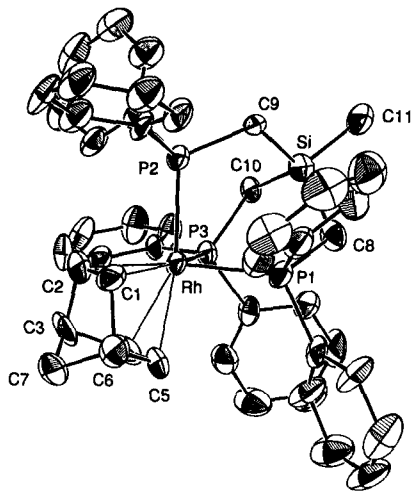

Fig. 1. An ORTEP view of the cation in [Rh(NBD)(MeSi(CH_2-PPh_2)$_3$)](OTf) (**14**).

the non-bonded interactions between the NBD ligands and the P atoms, is closely related to the change from the prevalently SPY structure of **16** to the prevalently TBP geometries of **14** and **15** as, after this rearrangement, the olefinic C1 and C2 atoms become coplanar with Rh, P1 and P3 in the TBP geometry (Fig. 1).

Finally, the possibility of a direct Sn–Rh interaction was considered. However, the distance between these two atoms in **15** is 3.858(3) Å and, therefore, it seems highly unlikely that such interaction occurs to any significant extent. A similar consideration applies to the Si–Rh interaction, the Si–Rh distance being 3.700(3) Å. Furthermore, the closing up of the C–E–C angles, on going from C to Si and Sn, speaks against an attractive interaction between rhodium and the bridgehead heteroatoms.

2.2.3. *Rhodium dicarbonyl complexes with ligands 4 and 5*

The reactivity of the ligand Si-triphos **4** is comparable with that of triphos **1** [6a]. The dicarbonyl–rhodium complex cation [Rh(CO)$_2$(Si-triphos)]$^+$ could be synthesized in good to excellent yields in several ways and was relatively stable in solution. Its salt [Rh(CO)$_2$(Si-triphos)][BPh$_4$] (**17**) was obtained by reacting [$Rh_2Cl_2(CO)_4$] with Si-triphos **4** in methanol solution under a CO atmosphere, followed by addition of Na[BPh$_4$]. In a similar way, [Rh(CO)$_2$(Si-triphos)](OTf) (**18**) was isolated from acetone, acetonitrile or dichloromethane solutions of [Rh(CO)$_2$(Si-triphos)]Cl after addition of silver or thallium triflate.

However, the Rh(I) carbonyl cation with the ligand Sn-triphos **5**, [Rh(CO)$_2$(Sn-triphos)]$^+$, could not be prepared as described above. This complex proved to be unstable in solution and its formation required the use of solvents which were saturated with CO. While the synthesis could be carried out in several solvents, isolation of the pure compound was not easy. Thus, attempts to precipitate the complex cation as its [BPh$_4$]$^-$ salt from a MeOH solution, using NH$_4$[BPh$_4$], resulted in the formation of significant amounts of oligomeric compounds. These were also formed when attempts were made to precipitate the complex as the triflate salt by reacting the chloro compound, in dichloromethane or acetone, with silver or thallium triflate. However, the desired product was obtained when [$Rh_2Cl_2(CO)_4$], in CH_2Cl_2, acetone or acetonitrile solution, was slowly added to a solution of ligand **5** and thallium triflate. The reaction was immediate; the thallium chloride formed was filtered off and the complex [Rh(CO)$_2$(Sn-triphos)](OTf) (**19**) was precipitated with Et_2O. The solid compound is air-stable in the solid state.

2.2.4. *Attempts to prepare Rh(I) complexes of 4 and 5 with other co-ligands*

The [Rh(I)(COD)] compounds (COD = 1,5-cyclooctadiene), analogous to the NBD complexes described above, could not be obtained: although the cationic complex [Rh(COD)(Si-triphos)]$^+$ was formed during the reaction between [$Rh_2Cl_2(COD)_2$] and Si-triphos **4**, it partly decomposed during attempts to isolate it.

The corresponding reaction with Sn-triphos **5** led mainly to the formation of oligomeric compounds, probably due to the larger size of COD. As mentioned above, the metal centres in complexes of ligands **4** and **5** are positioned more deeply in the cavity formed by

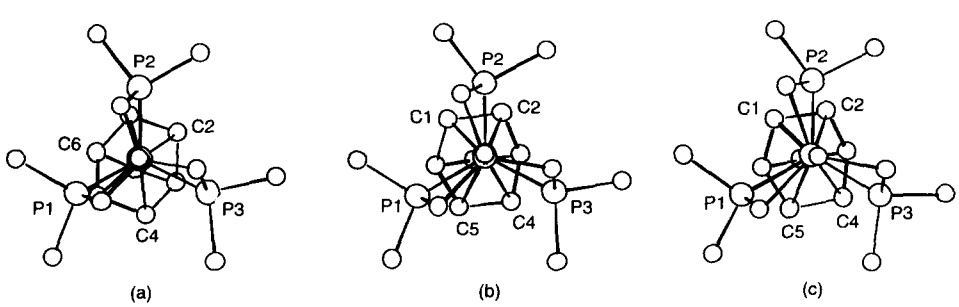

Fig. 2. Projections of the [Rh(NBD)(RE(CH_2PPh_2)$_3$)]$^+$ cations viewed along the E–Rh vector for **16** (a), **14** (b) and **15** (c). The $CH_3CH_2CH_2$ chain in **15** and the phenyl rings are omitted for clarity.

the ligands, so that the terminal phenyl groups partly block the remaining coordination sites, this effect being more evident in the case of the Sn-ligand **5**. Thus, while NBD is sufficiently small to allow the formation of stable complexes with both ligands **4** and **5**, only Si-triphos **4** forms a COD analogue which, however, is not sufficiently stable to be isolated.

Therefore, it can be concluded that, in the complexes containing the [Rh(tripod)] moieties as potential catalyst precursors, the presence of an Sn instead of a C atom at the top of the tripod skeleton, not only should allow the preparation of enantiopure C_3-symmetric fragments, but may also produce species with greater shielding of the metal centre, enhancing the effect of large substituents at the P atoms.

2.3. *The ruthenium complexes*

As Sn-triphos **5** appeared to exhibit donor properties which were significantly different from those of triphos **1** and Si-triphos **4**, the ruthenium(II) coordination chemistry of the former ligand was studied. It is well established that the reaction of chloro-containing precursors such as $[RuCl_2(dmso)_4]$ with triphod-like ligands leads to the formation of trichloro-bridged species [2d]. However, in the case of Sn-triphos **5** the formation of ruthenium(II) five-coordinated species of the type $[RuCl_2$(Sn-triphos)] might also be possible given the higher steric requirements of this ligand relative to those of triphos.

Recent investigations in this laboratory have shown that the binuclear species $[(COD)(CF_3CO_2)Ru(\mu\text{-}CF_3CO_2)_2Ru(CF_3CO_2)(COD)]$ [22] is a suitable precursor for the synthesis of mononuclear ruthenium(II) complexes containing tripod-like phosphine ligands [12f]. The COD ligand is smoothly replaced by this ligand, while the potentially bidentate trifluoroacetato anion promotes the formation of mononuclear, six-coordinate complexes. Moreover, the displacement of the trifluoroacetato ligands by protonation allows their easy substitution by a variety of either neutral or anionic ligands [12f]. Therefore, both $[Ru(O_2CCF_3)_2$(triphos)] (**20**) and $[Ru(O_2CCF_3)_2$(Sn-triphos)] (**21**) were prepared and their reactivity with acids in the presence of chloride ions studied.

2.3.1. *$[Ru(O_2CCF_3)_2$(triphos)] (20) and $[Ru(O_2CCF_3)_2$(Sn-triphos)] (21)*

The complexes $[Ru(O_2CCF_3)_2$(triphos)] (**20**) and $[Ru(O_2CCF_3)_2$(Sn-triphos)] (**21**) were prepared by reacting $[Ru_2(CF_3CO_2)_4(COD)_2]$ with the appropriate ligand in THF solution. The products are assigned six-coordinate structures, one trifluoroacetato anion acting as monodentate and the other as bidentate, as shown below, both in the solid state and in solutions of non-coordinating solvents, on the basis of: (i) their FAB^+ mass spectra which exhibit weak parent ions at *m/z* 952 and 1100, respectively; (ii) their molecular weights in CH_2Cl_2, determined by osmometry; (iii) their non-electrolyte nature in acetone solution; (iv) the values of their ^{31}P NMR chemical shifts in CD_2Cl_2 solution; (v) the yellow colours of the solids and the pale yellow colours of the $CDCl_3$ or CD_2Cl_2 solutions (all the previously reported five-coordinate ruthenium(II) complexes containing phosphine ligands exhibit either dark green or red–brown colours, depending on donor set and geometry [23]).

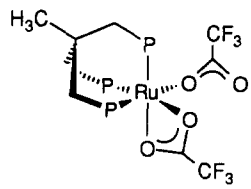

20

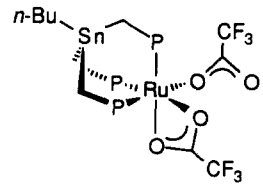

21

The temperature dependence of the ^{31}P and ^{19}F NMR solution spectra of both **20** and **21** suggests the occurrence of dynamic processes in solution consisting in an exchange between the mono- and the bidentate trifluoroacetato groups, which is fast on the NMR time-scale at room temperature. Accordingly, in the room-temperature ^{19}F NMR spectrum of **21**, the two trifluoroacetato ligands give rise to a single, sharp signal which broadens when the sample temperature is lowered and, at −100 °C, is resolved into two singlets of equal intensities at δ −76.0 and −76.4. These signals can be assigned to the mono- and bidentate trifluoroacetato groups [24].

The room-temperature ^{31}P NMR spectrum of **21** (a singlet at δ 40.1), upon lowering the sample temperature, broadens and eventually resolves into three distinct signals. The limiting spectrum, reached at −100 °C, corresponds to an AMX spin system whose ^{31}P chemical shift values and J(P,P) are consistent with a complex having *fac*-octahedral geometry [25]. The mean value of the shifts at −100 °C (42.4) is close to the room-temperature value, suggesting that the six-coordinate structure remains substantially unchanged in the temperature range studied.

The presence of three inequivalent P atoms in the low-temperature ^{31}P NMR spectra indicates that complex **21** has no symmetry element. While a C_s symmetry is expected for the structure proposed for **21**, when the orientations of the phenyl substituents on the P atoms are taken into account, the symmetry of the coordinated tripodal phosphine **5** can be lower than C_s. If the arrangement of the phenyl groups becomes rigid in solution, e.g. as the interconversion between the different conformers slows down, the apparent C_s symmetry of complex **21** is lost. Thus, the AMX ^{31}P NMR spectral pattern recorded for **21** at −100 °C can be explained by postulating that the interconversion of

enantiomeric conformers becomes slow at very low temperatures. Analogous symmetry reductions have been detected by low-temperature ^{31}P NMR spectra in some ruthenium(II) and osmium(II) complexes containing the diphosphine $(c\text{-}C_6H_{11})_2PCH_2CH_2P(c\text{-}C_6H_{11})_2$ [26]. These changes have been attributed to the slowing down of the ligand motions due to the steric interactions between the bulky substituents at the P atoms.

In the case of the triphos complex **20**, limiting spectra were not observed either by ^{31}P or ^{19}F NMR even at −100 °C, the lowest temperature which coud be reached. The failure to observe the low-exchange regime in this case is probably related to the lower steric demands of triphos **1**, compared to Sn-triphos **5**.

It should be noted that also the formation of a seven-coordinated structure with two bidentate CF_3COO^- anions might explain the fluxional behaviour observed both for **20** and for **21**, as such structures are known to be highly fluxional. This hypothesis is disfavoured as a seven-coordinated d^6 ruthenium(II) complex would be a 20 electron system. However, such a structure could be involved as a transition state in the interchange between the mono- and the bidentate trifluoroacetato groups.

2.3.2. *The reactivity of 20 and 21 with H_2O*

Complexes **20** and **21** readily react with water, a relatively weak donor. Thus, even after distillation over Pb/Na, the solvents used for NMR studies had to be carefully dried over molecular sieves. Variable-temperature ^1H and ^{31}P NMR studies suggest that the aqua complexes $[Ru(O_2CCF_3)_2(OH_2)(triphos)]$ (**22**) and $[Ru(O_2CCF_3)_2(OH_2)(Sn\text{-}triphos)]$ (**23**) with monodentate trifluoroacetato ligands, are formed when incompletely dry solvents are used (Eq. (3)). An analogous equilibrium, in which the change of the hapticity of a sulfonate ligand from bi- to monodentate accompanies the reversible association of a water molecule, has been proposed for $[M(O_3SR)(OH_2)(CO)(PPh_3)_2]$ (M = Ru or Os; R = Me, CF_3 or $p\text{-}C_6H_4Me$) [27a]. The isolation of **22** and **23** in the solid state was not attempted due to their lability (see below). However, the equilibrium shown in Eq. (3) was qualitatively investigated by variable-temperature NMR.

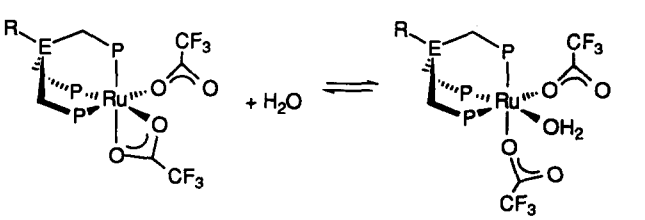

E = C, R = Me **20** E = C, R = Me **22**
E = Sn, R = *n*-Bu **21** E = Sn, R = *n*-Bu **23** (3)

When a threefold excess of H_2O is added to a CD_2Cl_2 solution of the triphos complex **20**, its room-temperature ^{31}P NMR spectrum exhibits a broad triplet and a broad doublet centred at δ 28.4 and 40.1, respectively. The limiting spectrum is reached at −20 °C and shows a well resolved AX_2 spin system whose δ ^{31}P and $J(P,P)$ values are consistent with complex **22**, having a *cis*-octahedral structure [25]. The ^{19}F NMR spectrum at −100 °C, showing a single resonance at δ −75.1, confirms the presence of two equivalent trifluoroacetato groups in **22**.

The ^{31}P NMR spectrum of a CD_2Cl_2 solution of **20**, to which less than 1 equiv. of H_2O is added, shows two broad signals at δ 28.4 and 40.4, which correspond to those of **22**, and a broad singlet at δ 41.7, attributed to **20**. By lowering the temperature to −20 °C, the signals of both **20** and **22** are observed. This suggests that the addition of H_2O is reversible and fast on the NMR time-scale. Furthermore, the addition of a molecular sieve to the above solution results in the disappearance of the signals due to **22** while the broad singlet due to **20** sharpens.

Evidence for the presence of a coordinated H_2O molecule in **22** comes from ^1H NMR studies. In addition to the signals of coordinated triphos **1**, the room-temperature ^1H NMR spectrum of the CD_2Cl_2 solutions of **20**, containing 3 equiv. of H_2O, shows a broad signal centred at δ 8.3, integrating approximately as 2 H atoms, attributed to the coordinated water molecule, and a broad signal at δ ~1.7 assigned to free H_2O. The signal at δ 8.3 sharpens and slightly moves to lower field as the temperature is lowered to −20 °C, indicating that equilibrium (3) slows down [28a,b].

The chemical shift of the H atoms of the coordinated H_2O molecule appears to be well outside the range observed for other ruthenium aqua complexes [28]. However, structure **22** is probably stabilized by intramolecular hydrogen bonds between the H_2O molecule and the monodentate trifluoroacetato ligands [27], as observed in *fac*-$[Ru(O_2CCF_3)_2(OH_2)(PMe_3)_3]$, which has the same coordination geometry as **22** and **23** [27c]. The involvement of the coordinated H_2O molecule in strong hydrogen bonds is expected to shift the δ value for the H atoms of coordinated water to lower field. Moreover, as only room-temperature ^1H NMR data are reported for some of the complexes [28c–f], it cannot be excluded that some of these chemical shift values might be affected by fast chemical exchange on the NMR time-scale between the coordinated H_2O molecule and traces of water in the solvents.

The assignment of the signal of the coordinated H_2O molecule was confirmed by a ^1H NMR presaturation experiment carried out at room temperature on a $CDCl_3$ solution of **20** containing 3 equiv. of H_2O. Irradiation of the signal of free H_2O at δ 1.7, before recording the spectrum, results in the disappearance of the signal of coordinated H_2O at δ 8.3. This indicates that the exchange between free and coordinated water is faster

than their relaxation process and confirms that equilibrium (3) is fast on the NMR time-scale. Furthermore, the signal of coordinated H_2O disappears upon addition of a large excess of D_2O.

Variable-temperature NMR studies show that the complex with Sn-triphos $[Ru(O_2CCF_3)_2(Sn\text{-triphos})]$ (**21**) behaves similarly to **20** and, apparently, adds water reversibly according to equilibrium (3) to give the adduct $[Ru(O_2CCF_3)_2(OH_2)(Sn\text{-triphos})]$ (**23**). The effects of the addition of a threefold excess of water to a CD_2Cl_2 solution of **21** was studied by ^{31}P, ^{19}F and ^1H NMR. The singlet in the ^{31}P NMR spectrum of the original solution is replaced by two broad resonances centred at δ 31.1 and 39.4 of relative intensities 1:1. The limiting spectrum, reached at −40 °C, corresponds to an AMX system analogous to that observed for **21** and, therefore, also in this case the conformational freedom of the phenyl rings is restricted at low temperature. The asymmetry of the molecule is confirmed by the observation of two ^{19}F resonances at −80 °C (δ −76.0 and −76.2), which coalesce into a single signal at δ −76.4 as the sample temperature is raised to 20 °C.

Unlike that of **20**, the room-temperature ^1H NMR spectrum of a solution of **21**, containing a threefold excess of water, does not show any signal attributable either to free or coordinated water. However, broad signals appear at δ 5.3 and 7.9 when the sample temperature is lowered to −20 °C and, at −40 °C, the exchange process appears to be frozen out: the signal at δ 7.9, integrating as 2 H atoms, is relatively sharp, while the signal due to free H_2O probably overlaps the methylene signals. As already found for **22**, addition of a molecular sieve to this CD_2Cl_2 solution shifts equilibrium (3) to the left and restores the spectral pattern of $[Ru(O_2CCF_3)_2(Sn\text{-triphos})]$ (**21**).

2.3.3. The reactivity of 20 and 21 with H^+ and chloride ions

Both trifluoroacetato ligands in the complex $[Ru(O_2CCF_3)_2(triphos)]$ (**20**) can be easily removed by adding protons to its CH_2Cl_2 solution in the presence of a large excess of chloride ions, e.g. by treating this solution either with (a) an excess of aqueous hydrochloric acid, followed by extraction of F_3CCOOH with water, or (b) $HBF_4 \cdot Et_2O$. These reactions give the known binuclear cation $[(triphos)Ru(\mu\text{-}Cl)_3Ru(triphos)]^+$ [2d]. The former method allowed the isolation of this cation as $[(triphos)Ru(\mu\text{-}Cl)_3Ru(triphos)][BPh_4]$ (**24**).

However, the analogous binuclear species $[(Sn\text{-triphos})Ru(\mu\text{-}Cl)_3Ru(Sn\text{-triphos})]^+$ could not be synthesized using either of these methods. The ^{31}P spectra of the solutions obtained as described above invariably showed the formation of a mixture of products, as indicated by the presence of a singlet at δ 28.6 and broad signals in the δ region 30–40. Method (b) gave the largest amounts of the product characterized by the singlet at δ 28.6. A FAB^+ mass spectrum of the orange solid obtained by evaporation of the solvent showed the most intense peak at *m/z* 911, which corresponds to the fragment $[RuCl(Sn\text{-triphos})]^+$. A weak signal at 1855, assignable to the fragment $[(Sn\text{-triphos})Ru(\mu\text{-}Cl)_3Ru(Sn\text{-triphos})]^+$, was also present. Both analytical and ^{31}P NMR data suggest that the materials obtained by either of the above methods are mixtures of products containing, in addition to variable amounts of $[(Sn\text{-triphos})Ru(\mu\text{-}Cl)_3Ru(Sn\text{-triphos})]^+$, which may give rise to the ^{31}P resonance at δ 28.6, other polynuclear species, probably of the composition $[RuCl_2(Sn\text{-triphos})]_x$. None of the solutions obtained from the protonation reactions in the presence of chloride ions gave significant amounts of mononuclear, five-coordinate $[RuCl_2(Sn\text{-triphos})]$, which is expected to be intensely coloured and to show ^{31}P NMR absorptions at lower fields than those of the six-coordinated complexes.

Although no pure product could be isolated as yet, these results suggest that the ruthenium(II) coordination chemistry of Sn-triphos **5** markedly differs from that of triphos **1** as the formation of a triply chloro-bridged product $[(Sn\text{-triphos})Ru(\mu\text{-}Cl)_3Ru(Sn\text{-triphos})]^+$ appears to be less favoured than with **1**. This is probably related to the different steric properties of Sn-triphos **5**, and in particular to the fact that, in its complexes, as mentioned earlier, the metal centre is more deeply embedded inside the tripod ligand cavity than is the case with either **4** or **1**. This structural feature would clearly disfavour the formation of binuclear species containing **5**, as the phenyl substituents of the two tripod moieties would get too close to each other in the binuclear complexes. However, although the steric bulk of the Sn-triphos ligand is higher than that of triphos, it is still not sufficient to stabilize a 16 electron, five-coordinated species such as $[RuCl_2(Sn\text{-triphos})]$. The latter probably associates forming the polynuclear species observed, the nature of which is presently under investigation in this laboratory.

3. Conclusions

The preparation of tripod-like ligands of the type $RSi(CH_2PR'R'')_3$, by reacting $RSiCl_3$ with $Li\text{-}CH_2P(BH_3)R'R''$, requires that at least one of the two terminal substituents R′ or R″ on the P atoms is an alkyl group. Such limitation is not observed for the formation of the $RSn(CH_2PR'R'')_3$ homologues.

The comparative studies of the coordinating properties of the homologous series of ligands **1**, **4** and **5** shows that a lengthening of the E–C bonds, as the central C atom is replaced first by silicon and then by tin, increases the steric crowding in the corresponding

complex cations present in **14** and **15**, respectively, and decreases the size of the active site(s) along the series C > Si > Sn. Furthermore, in the case of ruthenium(II), the tendency to form trihalo-bridged bimetallic complexes decreases in the same order.

4. Experimental

4.1. Equipment

Elemental analyses were performed by the 'Mikroelementaranalytisches Laboratorium der Eidgenössischen Technischen Hochschule Zürich'. FAB^+ mass spectra were carried out on a ZAB VSEQ instrument by the MS service of the Laboratorium für Organische Chemie (ETH Zürich) in a 3-NOBA (3-nitrobenzyl alcohol) matrix using an Xe-atom beam with a translational energy of 8 KeV. Melting points were obtained from samples in open capillary tubes with a Büchi SMP-20 melting point apparatus, and no corrections were applied. IR spectra were recorded on a Perkin-Elmer model 883 spectrophotometer. ^1H, $^{13}C\{^1H\}$ and $^{31}P\{^1H\}$ NMR spectra were measured on a Bruker WM 250 spectometer (250.1, 62.9 and 101.3 MHz); $^{19}F\{^1H\}$ spectra on a Bruker AC 200 spectometer (188.3 MHz). Chemical shifts are referenced to internal TMS (^1H and $^{13}C\{^1H\}$), external 85% H_3PO_4 ($^{31}P\{^1H\}$), and external neat $CFCl_3$ ($^{19}F\{^1H\}$). The J(SnH), J(SnP) and J(SnC) coupling constants of the unresolved satellites due to ^{117}Sn and ^{119}Sn are given when observed in the ^1H, $^{13}C\{^1H\}$ and $^{31}P\{^1H\}$ NMR spectra of the tin-containing compounds. Presaturation experiments were carried out using a standard microprogram from the Bruker library.

4.2. Syntheses

All reactions and manipulations were routinely performed under an atmosphere of argon by using Schlenk-type techniques. Diethyl ether (Et_2O) and tetrahydrofuran (THF) were distilled from sodium-benzophenone ketyl under nitrogen and toluene from $LiAlH_4$. Acetonitrile (CH_3CN) and dichloromethane (CH_2Cl_2) were distilled from CaH_2. All other chemicals of reagent grade were used as received. The starting materials PPh_2Me [29], $[Rh_2Cl_2(NBD)_2]$ [30] and $[Rh_2Cl_2(CO)_4]$ [31] were prepared as described in the appropriate reference. Flash chromatography (FC) was carried out on Fluka silica gel 60 (particle size 0.035–0.070; 220–440 mesh ASTM).

4.2.1. $MeP(BH_3)Ph_2$ (6)

To a stirred solution of PPh_2Me (31 g, 153 mmol), in degassed toluene (400 ml), $(CH_3)_2S \cdot H_3$ (15 ml, 158 mmol) was added at room temperature. After 2 h the solvent was removed under reduced pressure and the resulting pasty oil was subjected to flash chromatography with n-hexane/ethyl acetate (3:1) as the eluent. The phosphine borane **6** was isolated as a white crystalline solid (30.5 g, 92%). ^{31}P NMR ($CDCl_3$): δ 9.4. ^1H NMR ($CDCl_3$): δ 7.72–7.36 (m, 10H, aromatic), 1.86 (d, 3H, $^2J(PH) = 10.1$ Hz, PCH_3).

4.2.2. $Me_2Si(CH_2P(BH_3)Ph_2)_2$ (9)

A cyclohexane/n-hexane solution (98:2, 4.07 ml) of *sec*-BuLi (1.4 M, 5.70 mmol) was added dropwise to a THF solution (15 ml) of $MeP(BH_3)Ph_2$ (**6**) (1.11 g, 5.18 mmol) at −78 °C. After stirring for 2 h at −78 °C, Me_2SiCl_2 (0.31 ml, 2.59 mmol) was rapidly added by means of a syringe. The yellow solution was allowed to warm up to room temperature and stirred for 3 h. The reaction was quenched with 2 M HCl and the product repeatedly extracted with CH_2Cl_2. The combined extracts were washed with a K_2CO_3 solution, dried over $MgSO_4$ and the solvent evaporated under reduced pressure. The resulting pasty oil was recrystallized from Et_2O/hexane to give **9** as a white, crystalline solid (1.12 g, 90%). *Anal.* Calc. for $C_{28}H_{36}B_2P_2Si$: C, 69.45; H, 7.49. Found: C, 68.86; H, 7.49%. ^{31}P NMR ($CDCl_3$): δ 11.8 (br). ^1H NMR ($CDCl_3$): δ 7.70–7.26 (m, 20H, aromatic), 1.69 (d, 4H, $^2J(P,H) = 15.2$ Hz, CH_2), −0.10 (s, 6H, $SiCH_3$). ^{13}C NMR ($CDCl_3$): δ 132.1 (d, $^1J(PC) = 55.3$ Hz, C_{ipso}), 131.8 (d, $^2J(PC) = 9.6$ Hz, C_{ortho}), 131.0 (d, $^4J(PC) = 2.3$ Hz, C_{para}), 128.8 (d, $^3J(PC) = 23.5$ Hz, C_{meta}), 13.0 (d, $^1J(PC) = 24.7$ Hz, PCH_2Si), 0.54 (t, $^3J(PC) = 1.7$ Hz, $SiCH_3$).

4.2.3. $Ph_2Si(CH_2P(BH_3)Ph_2)_2$ (10)

A cyclohexane/n-hexane solution (98:2, 0.90 ml) of *sec*-BuLi (1.4 M, 1.26 mmol) was added dropwise to a THF solution (3 ml) of $MeP(BH_3)Ph_2$ (**6**) (244.5 mg, 1.14 mmol) at −78 °C. After stirring for 2 h at −78 °C, Ph_2SiCl_2 (0.12 ml, 0.57 mmol) was rapidly added by means of a syringe. The yellow solution was allowed to warm up to room temperature and stirred for 12 h. The reaction was quenched with 2 M HCl and the product extracted with CH_2Cl_2. The combined extracts were washed with a K_2CO_3 solution, dried over $MgSO_4$ and the solvent evaporated under reduced pressure. After purification by flash chromatography with n-hexane/ethyl acetate (4:1) as eluent, **10** was isolated as a white, crystalline solid (240 mg, 70%). *Anal.* Calc. for $C_{38}H_{40}B_2P_2Si$: C, 75.02; H, 6.63. Found: C, 74.04; H, 6.62%. ^{31}P NMR ($CDCl_3$): δ 14.2 (br). ^1H NMR ($CDCl_3$): δ 7.51–7.01 (m, 30H, aromatic), 2.53 (d, 4H, $^2J(P,H) = 15.2$ Hz, CH_2). ^{13}C NMR ($CDCl_3$): δ 135.6–127.4 (aromatic), 10.5 (d, $^1J(PC) = 24.8$ Hz, PCH_2Si).

4.2.4. $MeSi(OTf)_3$

To a solution of $Ph_2SiClCH_3$ (8.0 ml, 38 mmol) in toluene (8 ml), $HOSO_2CF_3$ (6.7 ml, 76 mmol) was slowly added at room temperature, and the yellow solution was stirred overnight. After evaporation of the solvent under reduced pressure, the resulting yellow liquid was distilled (b.p. 50 °C, 0.15 torr) to give $CH_3SiCl(OTf)_2$ (4.1 g, 29%). ^1H NMR ($CDCl_3$): δ 1.18 (s, CH_3). To a $CHCl_3$ solution (3 ml) of $CH_3SiCl(OTf)_2$ (3.2 g, 8.5 mmol) $AgOSO_2CF_3$ (2.2 g, 8.5 mmol) was added at room temperature. After stirring for 1 h, the AgCl precipitate was filtered off and the solvent removed in vacuo. The resulting pale yellow liquid was distilled (b.p. 75 °C, 0.15 torr) to give $CH_3Si(OTf)_3$ (3.0 g, 72%). ^1H NMR ($CDCl_3$): δ 1.23 (s, CH_3).

4.2.5. $MeSi(CH_2PPh_2)_3$ (4)

A solution of CH_3SiCl_3 (11.7 ml, 0.10 mol) and CH_2ClBr (21.4 ml, 0.32 mol) in dry THF (500 ml) was cooled at −78 °C, and n-BuLi (200 ml, 1.6 M in n-hexane, 0.32 mol) was added thereto over 1.5 h. The solution was allowed to warm up to room temperature over 2 h and stirred for 1 h. The reaction was quenched with water and the product was repeatedly extracted with n-hexane. The combined extracts were dried over $MgSO_4$ and the solvent evaporated under reduced pressure leaving a pale yellow oil. Its ^1H NMR spectrum showed that the reaction was not quantitative, as a significant amount (30%) of the chloromethyl disubstituted silane $MeSi(CH_2Cl)_2Cl$ was still present. The oil was carefully distilled under reduced pressure through a 20 cm Vigreux column. The main fraction (64–68 °C, 0.5 mm Hg) was a mixture of the expected $CH_3Si(CH_2Cl)_3$ and 10% of the disubstituted silane $CH_3SiCl(CH_2Cl)_2$, as shown by ^1H NMR. A second distillation through a 20 cm Vigreux column of the mixture did not lead to an enrichment of the product (8.4 g, 44%, calculated on the basis of $CH_3Si(CH_2Cl)_3$). ^1H NMR ($CDCl_3$): $CH_3Si(CH_2Cl)_3$: δ 3.03 (s, 6H, CH_2), 0.39 (s, 3H, CH_3). $CH_3SiCl(CH_2Cl)_2$: δ 2.91 (s, 4H, CH_2), 0.23 (s, 3H, CH_3).

A mixture of PPh_2Cl (18 ml, 97.4 mmol) and lithium granulate (1.49 g, 214 mmol), in dry degassed THF (300 ml), was stirred overnight at room temperature.

Table 2
Experimental data for the X-ray studies of **14**·Me_2CO and **15**·Et_2O

Compound	**14**·Me_2CO	**15**·Et_2O
Formula	$C_{51}H_{53}F_3O_4P_3RhSSi$	$C_{55}H_{63}F_3O_4P_3RhSSn$
Molecular weight	1042.96	1191.70
Crystal dimensions (mm)	0.40×0.30×0.40	0.20×0.20×0.18
Data collection T (°C)	23	23
Diffractometer	CAD4	R3m/v
Crystal system	monoclinic	monoclinic
Space group	$P2_1/n$	$P2_1/c$
a (Å)	12.069(2)	13.859(3)
b (Å)	29.865(5)	23.283(5)
c (Å)	14.086(6)	16.976(3)
β (°)	106.10(2)	101.12(3)
V (Å^3)	4878(1)	5375(2)
Z	4	4
ρ (calc.) (g cm^{-3})	1.420	1.472
μ (cm^{-1})	5.592	9.510
Radiation	Mo Kα (graphite monochromated, λ = 0.71069 Å)	
Measured reflections	$\pm h$, $+k$, $+l$	$\pm h$, $+k$, $+l$
θ Range (°)	$2.5<\theta<23.0$	$1.5<\theta<20.0$
Scan type	$\omega/2\theta$	$\omega/2\theta$
Scan width (°)	1.20+0.35 tan θ	1.20
Max. counting time (s)	90	40
Background time (s)	0.5×scan time	0.25×scan time
Max. scan speed (° min^{-1})	4.5	15.0
Prescan rejection limit	0.55 (1.82 σ)	
Prescan acceptance limit	0.025 (40 σ)	
No. independent data collected	6370	7025
No. observed reflections (n_o)	3790 ($\lvert F_o\rvert^2>3.0\sigma(\lvert F_o\rvert^2)$)	5324 ($\lvert F_o\rvert^2>4.0\sigma(\lvert F_o\rvert^2)$)
Transmission coefficient	0.842–0.994	
Decay correction	0.994–1.642	
No. parameters refined (n_v)	517	613
Δ_p/σ (Max. shift at convergence)	<0.25	<0.8
R [a]	0.072	0.060
R_w [a]	0.096	0.072

[a] $R=\Sigma\lvert\lvert F_o\rvert-(1/k)\lvert F_c\rvert\rvert/\Sigma\lvert F_o\rvert$, $R_w=[\Sigma w(\lvert F_o\rvert-(1/k)\lvert F_c\rvert)^2/\Sigma w\lvert F_o\rvert^2]^{1/2}$.

Table 3
Final positional and isotropic equivalent displacement parameters U (Å^2) for **14**·Me_2CO [a]

Atom	x	y	z	U_{eq} [a]
Rh	−0.22540(7)	−0.11432(3)	0.04433(6)	0.0420(4)
P1	−0.3236(3)	−0.880(1)	0.1624(2)	0.051(1)
P2	−0.3269(2)	−0.18116(9)	0.0198(2)	0.048(1)
P3	−0.0707(2)	−0.1485(1)	0.1689(2)	0.047(1)
Si	−0.2732(3)	−0.1842(1)	0.2463(2)	0.056(2)
C1	−0.316(1)	−0.0888(4)	−0.0992(8)	0.063(6)
C2	−0.220(1)	−0.1132(5)	−0.1091(8)	0.080(6)
C3	−0.126(1)	−0.0793(4)	−0.1027(8)	0.080(7)
C4	−0.100(1)	−0.0653(4)	0.0053(9)	0.076(7)
C5	−0.193(1)	−0.0414(4)	0.0120(8)	0.076(7)
C6	−0.275(1)	−0.0397(4)	−0.0881(9)	0.078(7)
C7	−0.194(1)	−0.0388(5)	−0.1529(9)	0.087(7)
C8	−0.2942(9)	−0.1238(4)	0.2719(8)	0.061(7)
C9	−0.3815(9)	−0.1974(4)	0.1236(8)	0.055(6)
C10	−0.1230(9)	−0.1938(4)	0.2329(8)	0.053(6)
C11	−0.299(1)	−0.2201(5)	0.3447(9)	0.091(7)
C15	−0.294(1)	−0.0323(4)	0.2171(7)	0.055(7)
C16	−0.181(1)	0.0175(4)	0.251(1)	0.087(7)
C17	−0.153(1)	0.0244(5)	0.294(1)	0.110(9)
C18	−0.239(2)	0.0530(5)	0.300(1)	0.112(9)
C19	−0.352(1)	0.0389(5)	0.269(1)	0.112(9)
C20	−0.381(1)	−0.0029(4)	0.224(1)	0.089(7)
C21	−0.480(1)	−0.0860(4)	0.1161(8)	0.066(7)
C22	−0.555(1)	−0.1046(5)	0.1664(9)	0.083(7)
C23	−0.672(1)	−0.1020(5)	0.126(1)	0.102(9)
C24	−0.718(1)	−0.0815(5)	0.037(1)	0.093(7)
C25	−0.647(1)	−0.0632(5)	−0.012(1)	0.089(7)
C26	−0.532(1)	−0.0652(4)	0.0248(9)	0.078(7)
C27	−0.453(1)	−0.1807(4)	−0.0883(7)	0.053(6)
C28	−0.560(1)	−0.1671(4)	−0.0812(8)	0.063(7)
C29	−0.652(1)	−0.1624(4)	−0.1669(9)	0.076(7)
C30	−0.638(1)	−0.1744(5)	−0.257(1)	0.083(8)
C31	−0.533(1)	−0.1875(4)	−0.2648(9)	0.080(7)
C32	−0.438(1)	−0.1915(4)	−0.1812(9)	0.078(6)
C33	−0.2540(9)	−0.2314(4)	−0.0075(8)	0.051(6)
C34	−0.300(1)	−0.2748(4)	0.000(1)	0.085(8)
C35	−0.247(1)	−0.3114(5)	−0.024(1)	0.099(9)
C36	−0.152(1)	−0.3067(5)	−0.058(1)	0.110(9)
C37	−0.106(1)	−0.2658(5)	−0.068(1)	0.103(9)
C38	−0.160(1)	−0.2280(4)	−0.0421(9)	0.068(7)
C39	0.0500(9)	−0.1751(4)	0.1350(7)	0.047(6)
C40	0.066(1)	−0.1677(4)	0.0418(8)	0.063(7)
C41	0.156(1)	−0.1898(5)	0.0149(9)	0.083(7)
C42	0.227(1)	−0.2175(5)	0.079(1)	0.091(7)
C43	0.214(1)	−0.2241(5)	0.175(1)	0.093(7)
C44	0.127(1)	−0.2027(5)	0.1994(9)	0.080(7)
C45	0.0138(9)	−0.1122(4)	0.2704(8)	0.055(5)
C46	0.091(1)	−0.0831(5)	0.2538(9)	0.076(7)
C47	0.153(1)	−0.0544(5)	0.325(1)	0.112(9)
C48	0.134(2)	−0.0562(5)	0.419(1)	0.118(9)
C49	0.063(1)	−0.0860(6)	0.4392(9)	0.097(9)
C50	0.002(1)	−0.1146(5)	0.3675(8)	0.072(7)
S	0.0114(5)	0.1697(2)	0.3175(5)	0.175(3)*
O1	−0.022(2)	0.155(1)	0.210(2)	0.34(1)*
O2	0.077(1)	−0.1495(6)	−0.357(1)	0.23(1)*
O3	−0.036(2)	−0.219(1)	−0.331(2)	0.32(1)*
C51	0.137(3)	0.139(1)	0.369(3)	0.28(2)*
F1	0.219(2)	0.1578(8)	0.343(2)	0.32(1)*
F2	−0.158(2)	−0.1432(7)	−0.468(2)	0.32(1)*
F3	−0.118(2)	−0.0971(9)	−0.353(2)	0.34(1)*
C52	0.443(5)	0.062(2)	0.510(5)	0.45(4)*
C53	0.325(4)	0.049(2)	0.506(3)	0.36(2)*
C54	0.468(3)	0.090(2)	0.414(3)	0.34(2)*
O4	0.483(3)	0.091(1)	0.578(3)	0.44(2)*

[a] Starred atoms were refined isotropically. Anisotropically refined atoms are given in the form of the isotropic equivalent displacement parameter U_{eq} defined as (1/3) of the trace of the orthogonalized U_{ij} tensor.

After filtering off the residual lithium, a solution of $CH_3Si(CH_2Cl)_3$, containing 10% of $CH_3SiCl(CH_2Cl)_2$, (6.22 g, 32 mmol calculated for $CH_3Si(CH_2Cl)_3$) in THF (150 ml) was added dropwise at −10 °C. The resulting suspension was allowed to warm up to room temperature and stirred for a further 3 h. The reaction was quenched with water and the product extracted with Et_2O. The organic layer was dried over $MgSO_4$ and the solvents were evaporated under reduced pressure. Recrystallization of the resulting pasty oil from MeOH gave Si-triphos **4** as a white, crystalline solid (14.3 g, 70%). *Anal.* Calc. for $C_{40}H_{39}P_3Si$: C, 74.98; H, 6.13. Found: C, 74.30; H, 6.01%. ^{31}P NMR ($CDCl_3$): δ −24.2 (s, $^2J(SiP)=15.4$ Hz). ^1H NMR ($CDCl_3$): δ 7.41–7.29 (m, 30H, aromatic), 1.23 (br s, 6H, PCH_2), −0.29 (s, 3H, $SiCH_3$). ^{13}C NMR ($CDCl_3$): δ 140.9 (d, $^1J(PC)=15.0$ Hz, C_{ipso}), 132.6 (d, $^2J(PC)=20.6$ Hz, C_{ortho}), 128.4 (s, C_{para}), 128.3 (d, $^3J(PC)=6.5$ Hz, C_{meta}), 13.7 (dt, $^1J(PC)=30.5$ Hz, $^4J(PC)=4.8$ Hz, PCH_2), −1.3 (q, $^3J(PC)=4.6$ Hz, $SiCH_3$).

4.2.6. *n-BuSn($CH_2P(BH_3)Ph_2)_3$ (13)*

To a solution of **6** (85.16 g, 24.10 mmol) in dry THF (70 ml), *sec*-BuLi (19 ml, 1.4 M in cyclohexane/n-hexane (98:2), 26.51 mmol) was added dropwise at −78 °C. After the addition was completed, the reaction mixture was stirred for a further 2 h at −78 °C. n-$BuSnCl_3$ (1.34 ml, 8.03 mmol) was then rapidly added by means of a syringe. The solution was allowed to warm up to room temperature, and stirred for 3 h. The reaction was quenched with 2 M HCl and the product was repeatedly extracted with CH_2Cl_2. The combined extracts were washed with a K_2CO_3 solution, dried over $MgSO_4$ and the solvents were evaporated. The pasty residual solid was recrystallized from Et_2O/n-hexane and gave **13** as a white, crystalline solid (5.7 g, 87%). M.p. 65 °C. *Anal.* Calc. for $C_{43}H_{54}B_3P_3Sn$: C, 63.37; H, 6.68. Found: C, 63.53; H, 6.88%. ^{31}P NMR ($CDCl_3$): δ 13.9 (br s). ^1H NMR ($CDCl_3$): δ 7.70–7.26 (m, 30H, aromatic), 1.60 (d, 6H, $^2J(PH)=13.0$ Hz, $^2J(SnH)=56.7$ Hz, PCH_2Sn), 0.85 (m, 4H, CH_2-β, CH_2-γ), 0.58 (t, 3H, $^3J(HH)=7.0$ Hz, CH_3), 0.44 (m, 2H, $SnCH_2$). ^{13}C NMR ($CDCl_3$): δ 132.5 (d, $^1J(PC)=54.7$ Hz, C_{ipso}), 131.7 (d, $^2J(PC)=9.6$ Hz, C_{ortho}), 131.2 (d, $^4J(PC)=2.0$

Table 4
Final positional and isotropic equivalent displacement parameters U_{eq} (Å^2) for **15**·Et_2O

Atom	x	y	z	U_{eq} [a]
Rh	0.1015(1)	0.5864(1)	0.3024(1)	0.045(1)
P1	0.2696(2)	0.5508(1)	0.3140(2)	0.051(1)
P2	0.1497(2)	0.6739(1)	0.3651(2)	0.048(1)
P3	0.0918(2)	0.6236(1)	0.1693(2)	0.050(1)
Sn	0.3078(1)	0.6804(1)	0.2471(1)	0.058(1)
C1	0.0526(9)	0.5535(5)	0.4041(8)	0.063(3)
C2	−0.0217(8)	0.5848(6)	0.3605(7)	0.058(3)
C3	−0.0887(9)	0.5422(5)	0.3086(8)	0.073(3)
C4	−0.0243(9)	0.5272(5)	0.2495(8)	0.062(3)
C5	0.0540(9)	0.4945(5)	0.2908(8)	0.060(3)
C6	0.035(1)	0.4903(5)	0.3767(8)	0.072(3)
C7	−0.079(1)	0.4885(6)	0.3619(9)	0.084(3)
C8	0.3408(8)	0.5903(5)	0.2544(7)	0.056(3)
C9	0.2707(9)	0.6954(5)	0.3630(7)	0.058(3)
C1	0.1660(8)	0.6868(4)	0.1675(6)	0.049(3)
C1	0.412(1)	0.7337(7)	0.2098(9)	0.101(3)
C1	0.430(1)	0.7153(9)	0.121(1)	0.162(3)
C1	0.499(2)	0.753(1)	0.086(2)	0.229(3)
C1	0.507(2)	0.727(1)	0.011(1)	0.292(3)
C1	0.2896(9)	0.4760(5)	0.2880(8)	0.055(3)
C1	0.307(1)	0.4621(6)	0.214(1)	0.096(3)
C1	0.319(1)	0.4047(8)	0.191(1)	0.129(3)
C1	0.315(1)	0.3618(6)	0.245(1)	0.103(3)
C1	0.297(1)	0.3742(6)	0.3183(9)	0.090(3)
C20	0.284(1)	0.4304(5)	0.3377(8)	0.073(3)
C21	0.3415(8)	0.5533(5)	0.4159(7)	0.048(3)
C22	0.4327(9)	0.5787(5)	0.4363(8)	0.058(3)
C23	0.4836(9)	0.5794(6)	0.5158(9)	0.071(3)
C24	0.444(1)	0.5541(6)	0.5759(8)	0.073(3)
C25	0.355(1)	0.5278(5)	0.5560(8)	0.067(3)
C26	0.3021(9)	0.5288(5)	0.4778(8)	0.057(3)
C27	0.143(1)	0.6735(5)	0.4722(7)	0.057(3)
C28	0.226(1)	0.6556(5)	0.5300(7)	0.072(3)
C29	0.213(1)	0.6528(5)	0.6101(8)	0.091(3)
C30	0.122(1)	0.6667(5)	0.6317(9)	0.088(3)
C31	0.044(1)	0.6843(6)	0.5756(8)	0.081(3)
C32	0.051(1)	0.6890(5)	0.4960(8)	0.070(3)
C33	0.0771(9)	0.7374(5)	0.3336(7)	0.052(3)
C34	0.111(1)	0.7936(5)	0.3556(7)	0.057(3)
C35	0.051(1)	0.8392(6)	0.3351(8)	0.072(3)
C36	−0.041(1)	0.8337(6)	0.2909(8)	0.076(3)
C37	−0.075(1)	0.7811(6)	0.2667(8)	0.072(3)
C38	−0.0185(9)	0.7324(6)	0.2895(7)	0.063(3)
C39	−0.0265(8)	0.6447(5)	0.1096(7)	0.046(3)
C40	−0.1129(9)	0.6428(5)	0.1386(7)	0.057(3)
C41	−0.2002(9)	0.6609(6)	0.0944(8)	0.067(3)
C42	−0.204(1)	0.6815(6)	0.0183(8)	0.071(3)
C43	−0.121(1)	0.6835(6)	−0.0123(8)	0.069(3)
C44	−0.0335(9)	0.6662(5)	0.0319(7)	0.059(3)
C45	0.1336(9)	0.5757(6)	0.0986(7)	0.058(3)
C46	0.099(1)	0.5213(7)	0.0886(9)	0.101(3)
C47	0.128(1)	0.4826(9)	0.039(1)	0.144(3)
C48	0.197(1)	0.5001(7)	−0.007(1)	0.113(3)
C49	0.235(1)	0.5538(8)	−0.0002(9)	0.112(3)
C50	0.201(1)	0.5912(7)	0.0517(8)	0.085(3)
S	0.3265(4)	0.3302(3)	0.6714(3)	0.123(2)
O1	0.340(1)	0.2700(6)	0.656(1)	0.202(3)
O2	0.258(1)	0.3444(7)	0.7169(8)	0.195(3)
O3	0.4167(9)	0.3607(6)	0.6789(8)	0.178(3)
C51	0.266(1)	0.3471(8)	0.571(1)	0.108(3)
C52	0.381(2)	0.625(1)	0.835(2)	0.135(3)
C53	0.379(3)	0.565(2)	0.806(2)	0.132(3)
C54	0.404(2)	0.490(2)	0.822(2)	0.118(3)
C55	0.440(2)	0.453(1)	0.889(2)	0.112(3)
O4	0.397(2)	0.531(2)	0.861(2)	0.169(3)
F1	0.244(1)	0.4035(5)	0.5665(7)	0.181(3)
F2	0.3206(8)	0.3384(6)	0.5192(7)	0.184(3)
F3	0.1809(8)	0.3222(5)	0.5535(8)	0.179(3)

[a] Isotropic equivalent displacement parameter U_{eq} defined as (1/3) of the trace of the the orthogonalized U_{ij} tensor.

Hz, C_{para}), 128.9 (d, ^3J(PC) = 10.0 Hz, C_{meta}), 27.9 (s, CH_2-β), 26.8 (s, CH_2-γ), 15.2 (s, CH_3), 13.4 (s, $SnCH_2$), 7.5 (d, ^1J(PC) = 24.4 Hz, PCH_2Sn). IR (KBr): ν(B–H) 2375 (s), 2330 (m), 2261 (w) cm^{-1}.

4.2.7. *n-BuSn(CH_2PPh_2)$_3$ (5)*

A solution of **13** (200 mg, 0.245 mmol) in morpholine (3 ml) was heated in a sealed tube for 2 h at 80 °C. The solvent was evaporated to dryness in vacuo and the resulting solid was recrystallized from CH_2Cl_2/propan-2-ol at −30 °C. At room temperature, **5** was a pasty colourless oil (148 mg, 78%). *Anal.* Calc. for $C_{43}H_{45}P_3Sn$: C, 66.77; H, 5.86. Found: C, 66.38; H, 5.93%. ^{31}P NMR ($CDCl_3$): δ −19.5 (s, ^2J(SnP) = 104.1 Hz). ^{1}H NMR ($CDCl_3$): δ 7.38–7.26 (m, 30H, aromatic), 1.12 (br s, 6H, PCH_2Sn), 1.01 (m, 4H, CH_2-β, CH_2-γ), 0.72 (t, 3H, ^3J(HH) = 6.7 Hz, CH_3), 0.38 (m, 2H, $SnCH_2$). ^{13}C NMR ($CDCl_3$): δ 141.8 (d, ^1J(PC) = 15.2 Hz, C_{ipso}), 132.4 (d, ^2J(PC) = 20.3 Hz, C_{ortho}), 128.4 (s, C_{para}), 128.3 (d, ^3J(PC) = 6.7 Hz, C_{meta}), 28.4 (s, CH_2-β), 27.0 (s, CH_2-γ), 13.5 (s, CH_3), 11.7 (s, $SnCH_2$), 6.9 (dt, ^1J(PC) = 33.5 Hz, ^3J(PC) = 4.2 Hz, PCH_2Sn).

4.2.8. *[Rh(NBD)(Si-triphos)](OTf) (14)*

A mixture of [$Rh_2Cl_2(NBD)_2$] (393 mg, 0.853 mmol) and [AgOTf] (438 mg, 1.71 mmol) was dissolved in degassed acetone (80 ml). The mixture was stirred for 30 min and then the silver chloride precipitate was allowed to settle. The pale yellow solution was reverse-filtered under argon into a solution of Si-triphos **4** (1.09 g, 1.71 mmol) in acetone (20 ml) at −78 °C. The resulting orange solution was allowed to warm up to room temperature, stirred for 1 h, and concentrated under reduced pressure to a volume of 50 ml. Upon addition of Et_2O, **14** was obtained as a yellow–orange crystalline solid which was filtered off and dried in vacuo (1.65 g, 98%). *Anal.* Calc. for $C_{48}H_{47}F_3O_3P_3SSiRh$: C, 58.54; H, 4.81. Found: C, 58.18; H, 5.14%. ^{31}P NMR ($CDCl_3$): δ 7.3 (d, ^1J(RhC) = 117.9 Hz). ^{1}H NMR ($CDCl_3$): δ 7.39–7.10 (m, 30H, aromatic), 3.79 (br s, 2H, bridgehead CH), 3.33 (br s, 4H, olefinic CH), 1.68 (br d, 6H, ^2J(PH) = 9.8 Hz, PCH_2), 1.35 (s, 2H, bridging

CH_2), 0.68 (s, 3H, $SiCH_3$). ^{13}C NMR ($CDCl_3$): δ 135.8 (m, C_{ipso}), 131.4 (m, C_{ortho}), 130.1 (br s, C_{para}), 128.9 (m, C_{meta}), 61.4 (br s, C_{bridge}), 47.6 (m, C_{olefin}), 46.4 (br s, $C_{bridgehead}$), 8.9 (br s, PCH_2), 0.01 (q, $^3J(PC)=7.0$, $SiCH_3$).

4.2.9. [Rh(NBD)(Sn-triphos)](OTf) (15)

Complex **15** was prepared and purified as described for **14** using $[Rh_2Cl_2(NBD)_2]$ (512 mg, 1.11 mmol) and [AgOTf] (571 mg, 2.22 mmol) in degassed acetone (80 ml) and n-$BuSn(CH_2PPh_2)_3$ (**1**) (1.72 g, 2.22 mmol) in acetone (20 ml). The yellow–orange crystalline complex was obtained in 90% yield. *Anal.* Calc. for $C_{51}H_{53}F_3O_3P_3SSnRh$: C, 54.81; H, 4.78. Found: C, 54.30; H, 4.89%. ^{31}P NMR ($CDCl_3$): δ 13.7 (d, $^1J(RhP)=119.6$ Hz). ^1H NMR ($CDCl_3$): δ 7.39–7.04 (m, 30H, aromatic), 3.66 (br s, 2H, bridgehead CH), 3.20 (br s, 4H, olefinic CH), 1.76 (m, 4H, CH_2-β, CH_2-γ), 1.67 (br d, 6H, $^2J(PH)=9.5$ Hz, PCH_2Sn), 1.41 (m, 2H, $SnCH_2$), 1.26 (br s, 2H, bridging CH_2), 0.94 (t, 3H, $^3J(HH)=7.3$ Hz, CH_3). ^{13}C NMR ($CDCl_3$): δ 137.1 (m, C_{ipso}), 131.1 (d, $^2J(PC)=1.6$ Hz, C_{ortho}), 129.7 (br s, C_{para}), 128.5 (br s, C_{meta}), 60.1 (br s, C_{bridge}), 47.5 (m, C_{olefin}), 45.8 (br s, $C_{bridgehead}$), 28.5 (s, $^2J(SnC)=29.1$ Hz, CH_2-β), 26.6 (s, $^3J(SnC)=67.5$ Hz, CH_2-γ), 14.3 (m, $^1J(SnC)=406.8$ Hz, $SnCH_2$), 13.6 (s, CH_3), 4.4 (br s, $^1J(SnC)=243.7$ Hz, PCH_2Sn).

4.2.10. [Rh(CO)$_2$(Si-triphos)][BPh$_4$] (17)

A solution of $[Rh_2Cl_2(CO)_4]$ (36.9 mg, 0.095 mmol) in MeOH (3 ml) was saturated with CO for 15 min. To the resulting yellow solution Si-triphos **4** (121.6 mg, 0.190 mmol) was added. The phosphine slowly dissolved and the solution became orange. The reaction mixture was stirred for 30 min under a CO atmosphere. Finally, the solution was cooled to 0 °C and $Na[BPh_4]$ (65 mg, 0.190 mmol) was added. After stirring for 1 h at 0 °C the yellow precipitate was filtered off, washed with MeOH and Et_2O, and dried in vacuo (200 mg, 95%). *Anal.* Calc. for $C_{66}H_{59}BO_2P_3SiRh$: C, 70.85; H, 5.31. Found: C, 70.48; H, 5.30%. ^{31}P NMR ($CDCl_3$): δ 5.5 (d, $^1J(RhP)=103.0$ Hz). ^1H NMR ($CDCl_3$): δ 7.46–7.01 (m, 50H, aromatic), 1.56 (d, 6H, $^2J(PH)=12.9$ Hz, PCH_2), 0.38 (br s, 3H, $SiCH_3$). ^{13}C NMR ($CDCl_3$): δ 194.9 (dq, $^1J(RhC)=56.8$ Hz, $^2J(PC)=23.2$ Hz, CO), 163.4 (q, $^1J(BC)=49.3$ Hz, BC_{ipso}), 136.5 (s, BPh_4), 133.9 (m, C_{ipso}), 131.0 (m, C_{ortho}), 130.8 (br s, C_{para}), 129.2 (m, C_{meta}), 125.5 (s, BPh_4), 121.6 (s, BPh_4), 7.2 (d, $^1J(PC)=4.3$ Hz, PCH_2), −0.2 (q, $^3J(PC)=7.2$ Hz, $SiCH_3$). IR (KBr): ν(C–O) 2055(s), 1979 (s) cm^{-1}. ν(B–C) 1578 (m), 611 (m) cm^{-1}.

4.2.11. [Rh(CO)$_2$(Si-triphos)](OTf) (18)

A solution of $[Rh_2Cl_2(CO)_4]$ (146.2 mg, 0.376 mmol) in CH_2Cl_2 (15 ml) was saturated with CO for 15 min. The resulting yellow solution was added to a CO-saturated solution of Si-triphos **4** (482 mg, 0.752 mmol) in CH_2Cl_2 (15 ml). The orange reaction mixture was stirred for 15 min under a CO atmosphere. Finally, [TlOTf] (266 mg, 0.752 mmol) was added and the suspension was stirred for a further 30 min. The thallium chloride precipitate was allowed to settle, and the reaction mixture was filtered under argon and concentrated under reduced pressure. The yellow product which precipitated on addition of Et_2O was filtered off and dried in vacuo (600 mg, 85%). *Anal.* Calc. for $C_{43}H_{39}F_3O_5P_3SSiRh$: C, 54.44; H, 4.14. Found: C, 54.58; H, 4.45%. ^{31}P NMR ($CDCl_3$): δ 6.2 (d, $^1J(RhP)=103.0$ Hz). ^1H NMR ($CDCl_3$): δ 7.31–7.15 (m, 30H, aromatic), 1.89 (d, 6H, $^2J(PH)=13.1$ Hz, PCH_2), 0.91 (q, 3H, $^4J(PH)=1.2$ Hz, $SiCH_3$). ^{13}C NMR ($CDCl_3$): δ 195.4 (dq, $^1J(RhC)=56.6$ Hz, $^2J(PC)=23.1$ Hz, CO), 134.3 (m, C_{ipso}), 131.0 (m, C_{ortho}), 130.6 (br s, C_{para}), 129.0 (m, C_{meta}), 7.2 (br s, PCH_2), −0.2 (q, $^3J(PC)=7.1$ Hz, $SiCH_3$). IR (RbI): ν(C–O) 2049 (s), 1975 (s) cm^{-1}.

4.2.12. Rh(CO)$_2$(Sn-triphos)](OTf) (19)

A CO-saturated solution of $[RhCl_2(CO)_4]$ (203 mg, 0.522 mmol) in CH_2Cl_2 (25 ml) was added to a suspension of Sn-triphos **5** (808 mg, 1.044 mmol) and [TlOTf] (369 mg, 1.044 mmol) in CH_2Cl_2 (25 ml), under a CO atmosphere. The resulting orange reaction mixture was stirred for 30 min. The thallium chloride precipitate was filtered off under argon and the solution was concentrated under reduced pressure to a volume of 25 ml. The yellow solid which precipitated upon addition of Et_2O was filtered off and dried in vacuo (850 mg, 75%). *Anal.* Calc. for $C_{46}H_{45}F_3O_5P_3SSnRh$: C, 51.09; H, 4.19. Found: C, 50.91; H, 4.31%. ^{31}P NMR ($CDCl_3$): δ 11.6 (d, $^1J(RhP)=104.4$ Hz). ^1H NMR ($CDCl_3$): δ 7.42–7.16 (m, 30H, aromatic), 1.81 (m, 4H, CH_2-β, CH_2-γ), 1.77 (br d, 6H, $^2J(PH)=12.4$ Hz, PCH_2Sn), 1.48 (m, 2H, $SnCH_2$), 1.02 (t, 3H, $^3J(HH)=7.3$ Hz, CH_3). ^{13}C NMR ($CDCl_3$): δ 194.9 (dq, $^1J(RhC)=56.7$ Hz, $^2J(PC)=23.4$ Hz, CO), 135.8 (m, C_{ipso}), 130.7 (d, $^2J(PC)=12.3$ Hz, C_{ortho}), 130.0 (br s, C_{para}), 128.5 (d, $^3J(PC)=10.0$ Hz, C_{meta}), 28.6 (s, $^2J(SnC)=31.4$ Hz, CH_2-β), 26.6 (s, $^3J(SnC)=67.4$ Hz, CH_2-γ), 16.6 (m, $SnCH_2$), 13.4 (s, CH_3), 2.6 (br s, $^1J(SnC)=235.8$ Hz, PCH_2Sn). IR (KBr): ν(C–O) 2050 (s), 1979 (s) cm^{-1}.

4.2.13. [Ru(O$_2$CCF$_3$)$_2$(triphos)] (20)

The complex $[Ru_2(O_2CCF_3)_4(COD)_2]$ (269 mg, 0.303 mmol) and the ligand triphos (378 mg, 0.605 mmol) were dissolved in THF (5 ml) and the resulting red–orange solution was heated at 60 °C for 2 h. The solvent was then evaporated under vacuum, the residue dissolved in CH_2Cl_2 (10 ml) and the resulting solution filtered over Celite. Evaporation of the solvent to dryness gave the analytically pure, yellow product (547 mg, 95%). *Anal.* Found: C, 56.74; H, 4.17; F, 11.71. Calc.: C, 56.79; H, 4.13; F, 11.98%. FAB^+ mass (m/z): 952

(M^+, 3%), 839 ($M^+ - O_2CCF_3$, 100%). $^{31}P\{^1H\}$ NMR (293 K, CD_2Cl_2, 101.3 MHz): δ 41.9 (s). $^{19}F\{^1H\}$ NMR (293 K, CD_2Cl_2, 188.3 MHz): δ −76.4 (s). ^1H NMR (293 K, CD_2Cl_2, 250 MHz): δ 7.61–7.01 (m, 30H, aromatic), 2.34 (m, 6H, PCH_2), 1.63 (q, 3H, $^4J(PH) = 2.9$ Hz, CH_3).

4.2.14. [Ru(O_2CCF_3)$_2$(Sn-triphos)] (21)

The complex [$Ru_2(O_2CCF_3)_4(COD)_2$] (223 mg, 0.250 mmol) and the ligand Sn-triphos **5** (408 mg, 0.528 mmol) were dissolved in THF (5 ml) and the resulting red–orange solution was heated at 60 °C for 12 h. The solvent was evaporated under vacuum and the orange residue, recrystallized from CH_2Cl_2/propan-2-ol/hexane, gave yellow microcrystals which were filtered off, washed with hexane, and dried under vacuum (410 mg, 75%). *Anal.* Found: C, 51.52; H, 4.04; F, 10.48. Calc.: C, 51.29; H, 4.12; F, 10.36%. FAB$^+$ mass (*m/z*): 1100 (M^+, 3%), 987 ($M^+ - O_2CCF_3$, 100%), 874 ($M^+ - 2O_2CCF_3$, 10%). $^{31}P\{^1H\}$ NMR (293 K, CD_2Cl_2, 101.3 MHz): δ 42.1 (s); 173 K: δ 40.1 [dd, 1P, $^2J(P,P')$ 37.6, $^2J(P,P'')$ 39.1 Hz], 42.0 [dd, 1P, $^2J(P'P'')$ 44.3 Hz], 45.1 [dd, 1P]. $^{19}F\{^1H\}$ NMR (293 K, CD_2Cl_2, 188.3 MHz): δ −76.1 (s); 173 K: δ −76.0 (s, 1F), −76.4 (s, 1F). ^1H NMR (CD_2Cl_2): δ 7.77–7.03 (m, 30H, aromatic), 1.81–1.56 (br m, 4H, CH_2-β, CH_2-γ), 1.61 (br d, 6H, $^2J(PH) = 5$ Hz, PCH_2Sn), 1.44 (m, 2H, $SnCH_2$), 1.01 (t, 3H, $^3J(HH) = 7.3$ Hz, CH_3).

4.2.15. [(Triphos)Ru(μ-Cl)$_3$Ru(triphos)][BPh$_4$] (24)

Aqueous concentrated HCl (0.33 ml, 4.0 mmol) was added to a CH_2Cl_2 solution (10 ml) of **20** (190 mg, 0.20 mmol) under stirring. After extraction of CF_3COOH and the excess of HCl with H_2O (10 ml) from the organic phase and drying over $MgSO_4$, an ethanol solution (2 ml) of Na[BPh_4] was added. After precipitation of NaCl, the solution was filtered over Celite and its volume was reduced. The resulting pale yellow precipitate was filtered off, washed with EtOH and dried in vacuo (140 mg, 75%). *Anal.* Found: C, 66.50; H, 5.38. Calc.: C, 67.83; H, 5.26%. FAB$^+$ mass (*m/z*): 1558 (M^+, 28%), 761 ([RuCl(triphos)]$^+$, 100%). The ^{31}P and ^1H NMR data of the cation of **24** are in agreement with those in the literature [2d].

4.3. Crystallography

Crystals of **14**·Me_2CO and **15**·Et_2O, suitable for X-ray diffraction analysis, were obtained by slow diffusion of Et_2O in an acetone solution of **14** and **15**, respectively.

Crystals of both compounds were mounted on glass fibres, at a random orientation, on an automated diffractometer for the unit cell and space group determinations and for the data collection. Unit cell dimensions were obtained by least-squares fit of the 2θ values of 25 high-order reflections ($9.8 < \theta < 14.5°$) for **14**·Me_2CO, and 20 reflections ($6.9 < \theta < 14.6°$) for **15**·Et_2O. Selected crystallographic and other relevant data are listed in Table 2.

Data were measured with variable scan speeds to ensure constant statistical precision on the collected intensities and corrected for Lorentz and polarization factors. An empirical absorption correction was also applied to the data of **14**·Me_2CO by using azimuthal (Ψ) scans of three 'high-χ' angle reflections. No extinction correction was deemed necessary for both structures.

The scattering factors used, corrected for the real and imaginary parts of the anomalous dispersion, were taken from the literature [32].

4.3.1. Crystal structure determination of 14·Me_2CO

A total of 6370 independent reflections was collected. During the data collection three standard reflections were measured every 60 min to check the stability of the crystal and of the experimental conditions. A decay correction was applied to the data set using the programs in the MOLEN crystallographic package [33]. The structure was solved by Patterson and Fourier methods and refined by full-matrix least-squares, the function minimized being $\Sigma w(F_o - 1/kF_c)^2]$, where $w = [\sigma^2(F_o)]^{-1}$ and $\sigma(F_o) = [\sigma^2(F_o^2) + 0.006(F_o^2)]^{1/2}/2F_o$ (k is the scale factor). Toward the end of the refinement a difference Fourier map revealed the presence of a clathrated acetone molecule that was included in the refinement. Anisotropic displacements parameters were used for the atoms of the complex cation except hydrogens, while both the OTf moiety and the acetone molecule were treated isotropically. The contribution of the H atoms, in calculated positions (C–H = 0.95 Å, $B_{CH} = 5.0$ Å^2), was taken into account but not refined. All calculations were carried out using the MOLEN crystallographic programs. Final atomic coordinates and equivalent isotropic displacement parameters are given in Table 3. A full numbering scheme for the cation is given in Fig. S2, see Section 5.

4.3.2. Crystal structure determination of 15·Et_2O

A set of 7025 independent reflections was collected. The stability of the crystal and of the experimental conditions was checked by measuring a standard every 200 reflections. Decay and absorption corrections were found to be unnecessary. The structure was solved by direct and Fourier methods and refined by full-matrix least-squares, the function minimized being $\Sigma w(F_o - 1/kF_c)^2]$ where $w = [\sigma^2(F_o)]^{-1}$ and $\sigma(F_o) = \sigma(F_o^2)/2F_o$. Toward the end of the refinement a difference Fourier map revealed the presence of a clathrated diethyl ether molecule. Anisotropic displacement parameters were used for all atoms except for the hydrogens the contribution of which was taken into account but not refined. The high displacement parameters of the C

atoms of the n-butyl group in **15** are not unexpected for a flexible, dangling alkyl chain. All calculations were carried out using the SHELXTL-PLUS programs [34]. Final atomic coordinates and equivalent isotropic displacement parameters are given in Table 4.

5. Supplementary material

An ORTEP view of the cation in **15** (Fig. S1); full numbering scheme for the cation in **14** (Fig. S2); tables of calculated positional parameters for the H atoms in **14**·Me_2CO (Table S1, 2 pages) and in **15**·Et_2O (Table S2, 3 pages); anisotropic displacement parameters for **14**·Me_2CO (Table S3, 2 pages) and for **15**·Et_2O (Table S4, 3 pages); extended list of bond lengths and angles in **14**·Me_2CO (Table S5, 5 pages) and in **15**·Et_2O (Table S6, 5 pages); listings of F_o and F_c for **14**·Me_2CO (Table S7, 22 pages) and for **15**·Et_2O (Table S8, 9 pages) are available on request from author A.A.

Acknowledgements

S.H. carried out the work during the tenure of a grant from the Swiss National Science Foundation and A.M. was supported by a Fellowship from the 'Forschungskommission' of the ETH Zürich. A.A. thanks MURST for financial support. The authors are indebted to one of the Referees for pointing out that the cations in **14** and **15** are best described as distorted trigonal bipyramids.

References

[1] (a) L. Sacconi and F. Mani, *Transition Met. Chem. (N.Y.), 8* (1982) 179; (b) C. Bianchini, C. Mealli, A. Meli and M. Sabat, in I. Bernal (ed.), *Stereochemistry of Organometallic and Inorganic Compounds*, Vol. 1, Elsevier, Amsterdam, 1986, p. 146.

[2] (a) C. Bianchini, C. Mealli, M. Peruzzini and F. Zanobini, *J. Am. Chem. Soc., 109* (1987) 5548; (b) M. Antberg and K.M. Frosin, *Chem. Ber., 121* (1988) 865; (c) C. Bianchini, D. Masi, A. Meli, M. Peruzzini and F. Zanobini, *J. Am. Chem. Soc., 110* (1988) 6411; (d) L.F. Rhodes, C. Sorato, L.M. Venanzi and F. Bachechi, *Inorg. Chem., 27* (1988) 604.

[3] W. Hewertson and H.R. Watson, *J. Chem. Soc.*, (1963) 1490.

[4] (a) J. Chatt and H.R. Watson, *J. Chem. Soc.*, (1961) 4980; (b) J. Chatt, F.A. Hart and H.R. Watson, *J. Chem. Soc.*, (1962) 2537; (c) J. Chatt and F.A. Hart, *J. Chem. Soc.*, (1965) 812.

[5] (a) C. Bianchini, C. Mealli, A. Meli, M. Peruzzini and F. Vizza, *Phosphorus, Sulfur, Silicon, 49/50* (1990) 425; (b) D.J. Rauscher, E.G. Thaler, J.C. Huffman and K.G. Caulton, *Organometallics, 10* (1991) 2209; (c) C. Bianchini, A. Meli, M. Peruzzini, A. Vacca, F. Vizza and A. Albinati, *Inorg. Chem., 31* (1992) 3841; (d) C. Bianchini, P. Barbaro, A. Meli, M. Peruzzini, A. Vacca and F. Vizza, *Organometallics, 12* (1993) 2505.

[6] (a) J. Ott, *Dissertation No. 8000,* ETH-Zürich, Switzerland, 1986; (b) C. Bianchini, A. Meli, F. Laschi, J.A. Ramirez, P. Zanello and A. Vacca, *Inorg. Chem., 27* (1988) 4429.

[7] (a) G.B. Consiglio, in J. Ott, *Dissertation No. 8000,* ETH-Zürich, Switzerland, 1986; (b) C. Bianchini, A. Meli, M. Peruzzini, F. Vizza, P. Frediani and J.A. Ramirez, *Organometallics, 9* (1990) 226; (c) E.G. Thaler, K. Folting and K.G. Caulton, *J. Am. Chem. Soc., 112* (1990) 2664.

[8] (a) J. Ott, G.M. Ramos Tombo, B. Schmid, L.M. Venanzi, G. Wang and T.R. Ward, *Tetrahedron Lett., 30* (1989) 6151; (b) *New J. Chem., 14* (1990) 495.

[9] (a) C. Bianchini, C. Mealli, A. Meli, D.M. Proserpio, M. Peruzzini, F. Vizza and P. Frediani, *J. Organomet. Chem., 369* (1989) C6; (b) C. Bianchini, A. Meli, M. Peruzzini and F. Vizza, *J. Am. Chem. Soc., 112* (1990) 6726; (c) P. Barbaro, C. Bianchini, C. Mealli and A. Meli, *J. Am. Chem. Soc., 113* (1991) 3181; (d) P. Barbaro, C. Bianchini, P. Frediani, A. Meli and F. Vizza, *Inorg. Chem., 31* (1992) 1523.

[10] (a) C. Bianchini, P. Frediani, A. Meli, F. Vizza, M. Peruzzini and F. Zanobini, *Organometallics, 8* (1989) 2080; (b) C. Bianchini, D. Masi, A. Meli, M. Peruzzini, A. Vacca, F. Laschi and P. Zanello, *Organometallics, 10* (1991) 636; (c) C. Bianchini, A. Meli, M. Peruzzini, A. Vacca and F. Vizza, *Organometallics, 10* (1991) 645; (d) C. Bianchini, K.G. Caulton, C. Chardon, O. Eisenstein, K. Folting, T.J. Johnson, A. Meli, M. Peruzzini, D.J. Rauscher, W.E. Streib and F. Vizza, *J. Am. Chem. Soc., 113* (1991) 5127.

[11] (a) C. Bianchini, A. Meli, M. Peruzzini, F. Vizza, P. Frediani, V. Herrera and R.A. Sanchez-Delgado, *J. Am. Chem. Soc., 115* (1993) 2731; (b) *115* (1993) 7505.

[12] (a) T.R. Ward, *Dissertation No. 9513,* ETH-Zürich, Switzerland, 1991; (b) M.J. Burk, J.E. Feaster and R.L. Harlow, *Tetrahedron: Asymmetry, 2* (1991) 569; (c) T.R. Ward, L.M. Venanzi, A. Albinati, F. Lianza, T. Gerfin, V. Gramlich and G.M. Ramos Tombo, *Helv. Chim. Acta, 74* (1991) 983; (d) O. Walter, T. Klein, G. Huttner and L. Zsolnai, *J. Organomet. Chem., 458* (1993) 63; (e) S. Herold, *Dissertation No. 10443,* ETH-Zürich, Switzerland, 1993; (f) A. Mezzetti and L.M. Venanzi, *Xth FECHEM Conf. Organometallic Chemistry, Crete, 1993,* p. 138.

[13] (a) J.K. Whitesell, *Chem. Rev., 89* (1989) 1581; (b) B. Bosnich (ed.), *Asymmetric Catalysis*, Martinus Nijhoff, Dordrecht, Netherlands, 1986; (c) J.D. Morrison (ed.), *Asymmetric Synthesis*, Vol. 5, Academic Press, Orlando, FL, 1985; (d) W.S. Knowles, *Acc. Chem. Res., 16* (1983) 106; (e) H.J. Brunner, *J. Organomet. Chem., 300* (1986) 39; (f) U. Nagel and B. Rieger, *Organometallics, 8* (1989) 1534.

[14] T. Imamoto, T. Oshiki, T. Onozawa, T. Kusumoto and K. Sato, *J. Am. Chem. Soc., 112* (1990) 5244.

[15] D.A. Armitage, in G. Wilkinson (ed.), *Comprehensive Organometallic Chemistry*, Vol. 2, Pergamon, Oxford, 1982, p. 9.

[16] (a) W. Uhlig, *J. Organomet. Chem., 409* (1991) 377; (b) A. R. Bassindale and T. Stout, *J. Organomet. Chem., 271* (1984) C1; (c) M. Schmeisser, P. Sartori and B. Lippsmeier, *Chem. Ber., 103* (1970) 868; (d) M. Riediker and W. Graf, *Helv. Chim. Acta, 62* (1979) 205.

[17] R. Noyori, S. Murata and M. Suzuki, *Tetrahedron, 37* (1981) 3899; P.J. Stang, M. Hanack and L.R. Subramanian, *Synthesis*, (1982) 85.

[18] (a) T. Kobayashi and K.H. Pannell, *Organometallics, 9* (1990) 2201; (b) T. Kobayashi and K.H. Pannell, *Organometallics, 10* (1991) 1960.

[19] F. Bachechi, J. Ott and L.M. Venanzi, *Acta Crystallogr., Sect. C, 45* (1989) 724.

[20] A.R. Rossi and R. Hoffman, *Inorg. Chem., 14* (1975) 365.

[21] A.G. Orpen, L. Brammer, F.H. Allen, O. Kennard, D.G. Watson and R. Taylor, *J. Chem. Soc., Dalton Trans.*, (1989) S1.

[22] M.O. Albers, D.C. Lilies, E. Singleton and J.A. Yates, *J. Organomet. Chem., 272* (1984) C62.

[23] (a) M. Schröder and T.A. Stephenson, in G. Wilkinson (ed.), *Comprehensive Coordination Chemistry*, Vol. 4, Pergamon, Oxford, 1987, p. 376; (b) E.A. Seddon and K.R. Seddon, *The Chemistry of Ruthenium*, Elsevier, Amsterdam, 1984, p. 487.

[24] A. Dobson and S.D. Robinson, *Inorg. Chem.*, *16* (1977) 137.

[25] P.S. Pregosin and R.W. Kunz, in P. Diehl, E. Fluck and R. Kosfeld (eds.), *NMR: Basic Principles and Progress*, Springer, Berlin, 1979.

[26] (a) A. Mezzetti, A. Del Zotto, P. Rigo and N. Bresciani Pahor, *J. Chem. Soc., Dalton Trans.*, (1989) 1045; (b) A. Mezzetti, A. Del Zotto, P. Rigo and E. Farnetti, *J. Chem. Soc., Dalton Trans.*, (1991) 1525.

[27] (a) P.A. Harding and S.D. Robinson, *J. Chem. Soc., Dalton Trans.*, (1988) 415; (b) P.A. Harding, M. Preece, S.D. Robinson and K. Henrick, *Inorg. Chim. Acta*, *118* (1986) L31; (c) M.O. Albers, D.C. Liles and E. Singleton, *Acta Crystallogr., Sect. C*, *43* (1987) 860;

[28] (a) Y. Sun, N.J. Taylor and A.J. Carty, *Inorg. Chem.*, *32* (1993) 4457; (b) A.J. Deeming, G.P. Proud, H.M. Dawes and M.B. Hursthouse, *J. Chem. Soc., Dalton Trans.*, (1986) 2545; (c) M. Esteruelas, F.J. Lahoz, J.A. Lopez, L.A. Oro, C. Schlünken, C. Valero and H. Werner, *Organometallics*, *11* (1992) 2034; (d) P.W. Blosser, J.C. Gallucci and A. Wojcicki, *Inorg. Chem.*, *31* (1992) 2376; (e) O.H. Bailey and A. Ludi, *Inorg. Chem.*, *24* (1985) 2582; (f) S.M. Boniface, G.R. Clark, T.J. Collins and W.R. Roper, *J. Organomet. Chem.*, *206* (1981) 109.

[29] V. Bianco and S. Doronzo, *Inorg. Synth.*, *16* (1976) 157.

[30] G. Giordano and R.H. Crabtree, *Inorg. Synth.*, *19* (1979) 219.

[31] R. Cramer, *Inorg. Synth.*, *15* (1974) 17.

[32] *International Tables for X-Ray Crystallography*, Vol. IV, Kynoch, Birmingham, UK, 1974.

[33] *MOLEN: Molecular Structure Solution Procedure*, Enraf-Nonius, Delft, Netherlands, 1987.

[34] G.M. Sheldrick, *SHELXTL-PLUS-88, Structure Determination Software Programs*, Nicolet Instrument Corp., Madison, WI, 1988.